Building and Environment 195 (2021) 107733

Contents lists available at ScienceDirect

Building and Environment

journal homepage: www.elsevier.com/locate/buildenv

# Vegetation cover and plant-trait effects on outdoor thermal comfort in a tropical city

Naika Meili [a,b,*], Juan Angel Acero [a,c], Nadav Peleg [b], Gabriele Manoli [d], Paolo Burlando [b], Simone Fatichi [e]

[a] Future Cities Laboratory, Singapore-ETH Centre, 1 Create Way, 138602, Singapore
[b] Institute of Environmental Engineering, ETH Zurich, Stefano Franscini-Platz 5, 8093 Zürich, Switzerland
[c] CENSAM, Singapore-MIT Alliance for Research and Technology, 1 Create Way, 138602, Singapore
[d] Department of Civil, Environmental and Geomatic Engineering, University College London, London WC1E 6BT, United Kingdom
[e] Department of Civil and Environmental Engineering, National University of Singapore, 1 Engineering Drive 2, 117576, Singapore

ARTICLE INFO

*Keywords:*
Outdoor thermal comfort
UTCI
Urban vegetation
Ecosystem services
Heat mitigation in the tropics
Urban ecohydrological model

ABSTRACT

An increase in urban vegetation is an often proposed mitigation strategy to reduce urban heat and improve outdoor thermal comfort (OTC). Vegetation can alter urban microclimate through changes in air temperature, mean radiant temperature, humidity, and wind speed. In this study, we model how street tree and ground vegetation cover and their structural, optical, interception, and physiological traits control the diurnal cycle of OTC in different urban densities in a tropical city (Singapore). For this purpose, we perform a variance based sensitivity analysis of the urban ecohydrological model UT&C. Model performance is evaluated through a comparison with local microclimate measurements and OTC is assessed with the Universal Thermal Climate Index (UTCI).

We find a pronounced daily cycle of vegetation effects on UTCI. Tree cover fraction is more efficient in decreasing UTCI during daytime, while a higher vegetated ground fraction provides more cooling during night. Generally, increasing vegetation cover fractions do not deter OTC, except in certain urban densities during some periods of the day. An increase in tree and ground vegetation fractions provides a higher average UTCI reduction compared to a change in vegetation traits (0.9 – 2.9 °C vs. 0.7 – 1.1 °C during midday, 10 month average). The increase in humidity related to plant transpiration prevents further reduction of UTCI. However, the choice of vegetation traits enhancing tree transpiration can decrease UTCI during hot periods. These results can inform urban planners on the selection of vegetation amount and traits to achieve feasible OTC improvements in tropical cities.

## 1. Introduction

The number of people living in urban areas is increasing globally, and especially cities in Asia and Africa are foreseen to grow rapidly in the coming years [1]. Increasing urbanization, combined with the projected rise in global temperature due to climate change [2], is likely to further elevate temperatures in cities [2–5] with potential adverse effects on the outdoor thermal comfort (OTC) of their inhabitants [2,6,7]. To reduce urban heat stress and improve OTC of city dwellers, increasing urban vegetation cover is an often proposed mitigation strategy [8–11]. Urban vegetation influences the urban climate during daytime as well as nighttime [10], during average climatic conditions as well as during heat waves [12], and requires planting, continuous maintenance, and possibly irrigation — all factors that have associated costs [13].

In several cases, such as in tropical hot humid cities, the effects of vegetation on OTC are not straightforward to predict. OTC is influenced by climatic variables, such as air temperature, relative humidity, mean radiant temperature, and wind speed [14–17], as well as human behaviour, clothing, acclimatisation, activity levels, and personal perception [18–21]. While vegetation can decrease air temperature and reduce mean radiant temperature through shade provision during certain hours of the day, benefiting OTC in hot cities [22,23], plants transpire and increase humidity which might deter OTC in humid climates [22]. Furthermore, vegetation can shelter and block wind

* Corresponding author at: Future Cities Laboratory, Singapore-ETH Centre, 1 Create Way, 138602, Singapore.
*E-mail addresses:* meili@ifu.baug.ethz.ch (N. Meili), juanangel@smart.mit.edu (J.A. Acero), nadav.peleg@sccer-soe.ethz.ch (N. Peleg), g.manoli@ucl.ac.uk (G. Manoli), paolo.burlando@ifu.baug.ethz.ch (P. Burlando), ceesimo@nus.edu.sg (S. Fatichi).

https://doi.org/10.1016/j.buildenv.2021.107733
Received 21 September 2020; Received in revised form 14 February 2021; Accepted 16 February 2021
Available online 22 February 2021

flow, which could further reduce OTC in warm and calm-windless locations [22].

In tropical cities, which are characterized by high temperatures year-round, low diurnal temperature range, as well as high night time humidity [24], this trade-off of temperature decrease and humidity increase needs to be properly analysed to evaluate the overall benefits of urban vegetation. OTC should be quantified throughout the diurnal cycle as well as under different climatic conditions with a comprehensive thermal comfort index [25], which is sensitive to humidity changes, such as the Universal Thermal Climate Index (UTCI) [15] or the Modified Physiologically Equivalent Temperature (mPET) [26].

Not only vegetation amount and type, such as grass or trees, can influence the effects of urban vegetation on OTC, but also vegetation structural, optical, interception, and physiological traits [10,27]. Plant-traits identifies morphological, anatomical, biochemical, physiological and phenological features of plant individuals [28] and are influenced by the choice of vegetation species. In land surface models, plant traits are defined through a set of parameters [27,29,30], which can influence simulation outputs [31]. A systematic sensitivity analysis can quantify the expected effects of certain vegetation traits, such as vegetation structure, interception capacity, albedo, and physiology on the OTC, for varying combinations of vegetation types and amount. Hence, numerical models offer the opportunity to identify vegetation amount and traits that provide the highest possible enhancement of OTC. Such knowledge is fundamental to guide and inform urban planners and landscape designers on the selection of plant species and vegetation cover, as well as set expectations within the limits of attainable OTC improvements.

Furthermore, a systematic sensitivity analyses can identify important model parameters [31], which need to be specified carefully, due to their impact on model outputs. While information on urban form and composition is readily available nowadays for many cities [32,33], it can be hard to determine the accurate values of vegetation parameters for a given urban environment, as they depend on plant species, age, and environmental and management conditions. Hence, knowledge on parameter sensitivity can be beneficial to concentrate efforts in model parameter estimation.

The urban ecohydrological model, Urban Tethys-Chloris (UT&C) [27], is currently one of the few models that is able to assess the impacts of vegetation physiology on urban climate [27,29]. UT&C includes a large set of parameters, specifying vegetation amount, structure, optical properties, canopy interception, and plant physiology. Using UT&C to simulate OTC in different urban densities, this study aims to answer the following questions: (i) which vegetation properties are the most influential in modifying OTC in humid tropical climates? (ii) Are there substantial differences in the effects of vegetation types and properties across hours of the day or during the hottest periods of the year? The city of Singapore is used as an exemplary case-study; model performance is assessed in five different locations with varying urban density and green cover.

## 2. Methods

### 2.1. Urban Tethys-Chloris (UT&C) and outdoor thermal comfort

The urban ecohydrological model UT&C is based on a combination of an urban canyon scheme and an ecohydrological model [27]. The average urban form at the neighbourhood scale is defined with the area averaged building height ($H_{can}$), canyon width ($W_{can}$), and roof width ($W_{roof}$) (see Fig. 1). The building height variability, used in the formulation of the urban aerodynamic roughness and displacement height [34,35], is defined by the maximum building height ($H_{can,max}$) and building height variability ($H_{can,std}$). UT&C includes street tree ($\lambda_{Tree}$) and ground vegetation ($\lambda_{G,veg}$) plan area fractions within the canyon (Fig. 1), and their structural, optical, interception, and physiological properties (Table 1). UT&C accounts for the interaction of urban vegetation with radiation, such as for example shade provision by trees [36] or modification of urban albedo. It calculates transpiration based on environmental conditions and plant photosynthetic activity [27,36], which is an important factor to determine the evapotranspirative responses and impacts of urban vegetation on relative humidity and, therefore, OTC. UT&C further includes the interception of precipitation on plant canopies and the infiltration of water into the soil column underneath vegetation. The model calculates wind speed at any height z, $Ws(z)$, combining a logarithmic and exponential wind profile above and within the urban canyon [37,38], which accounts for average urban geometry and tree cover [34,35]. Through these processes, influenced by the properties of vegetation, the effects of different vegetation types and traits on the urban micro climate and hydrology can be modelled, as well as the feedback of the urban environment on plant performance [36].

UT&C calculates the 2 $m$ air temperature $T_{2m}$, 2 $m$ humidity $RH_{2m}$, and the urban and vegetation surface temperatures as a solution of the urban energy and water budget [27]:

$$R_n + Q_f = H + \lambda E + G \quad (1)$$

$$P + Ir = R + E + Lk + \Delta S \quad (2)$$

where $R_n$ is the net short- and longwave radiation [W m$^{-2}$], $Q_f$ the anthropogenic heat flux [W m$^{-2}$], $H$ the sensible heat flux [W m$^{-2}$], $\lambda E$ the latent heat flux [W m$^{-2}$], which is calculated as the product of evapotranspiration $E$ [kg m$^{-2}$ s$^{-1}$] and the latent heat of vaporization $\lambda$ [J kg$^{-1}$], $G$ the conductive heat flux including heat storage effects [W m$^{-2}$], $P$ the precipitation [kg m$^{-2}$ s$^{-1}$], $Ir$ the water input through irrigation [kg m$^{-2}$ s$^{-1}$], $R$ the surface runoff [kg m$^{-2}$ s$^{-1}$], $Lk$ the deep leakage at the bottom of the soil column [kg m$^{-2}$ s$^{-1}$], and $\Delta S$ the change in water storage [kg m$^{-2}$ s$^{-1}$]. The detailed description of the UT&C model process formulation and $T_{2m}$, $RH_{2m}$, and $Ws$ calculation can be found in [27] and its accompanying technical reference material. The calculation of mean radiant temperature $T_{mrt}$ is introduced in this article and described in the Supplementary Information A.

UT&C assesses OTC using UTCI [15], which is calculated using the polynomial regression described in [14,39], as a function of the simulated $T_{2m}$, $RH_{2m}$, $T_{mrt}$ and $Ws_{10m}$ [14]. UTCI is one of the four OTC indices identified as suitable for human biometeorological assessment by [25] as it provides an equivalent air temperature and is based on the energy budget model of a human body.

### 2.2. Case study: Singapore

The city of Singapore is chosen as a case study in this work due to its representative tropical climate (Köppen classification: Af) with high air temperatures, high relative humidity, and abundant rainfall year round [40]. Additionally, Singapore has a wealth of past studies analysing and modelling its urban climate, heat island, and OTC [e.g.,5,22,41], which leads to the availability of high-quality data, such as a high resolution land cover and building height map [33], and energy flux measurements of an eddy-covariance tower [40,42]. Using these eddy-covariance measurements, UT&C's model performance at the neighbourhood scale was previously evaluated in Singapore through the comparison of simulated and measured energy fluxes of net radiation, sensible heat, and latent heat, which showed good model performance in the tropical context [27]. In this study, UT&C's performance is further assessed against microclimate variables influencing OTC in Singapore.

#### 2.2.1. Meteorological and microclimate measurements

Near pedestrian level microclimate variables ($T_{2m}$, $RH_{2m}$, $Ws_{2m}$, $T_{mrt}$) were measured at five locations with varying urban density and vegetation cover in the city centre of Singapore (Fig. 2). The measurement campaign included three sites in dense low to mid-rise urban settings: (1) Boon Tat St. without vegetation cover, (2) Duxton3 with a

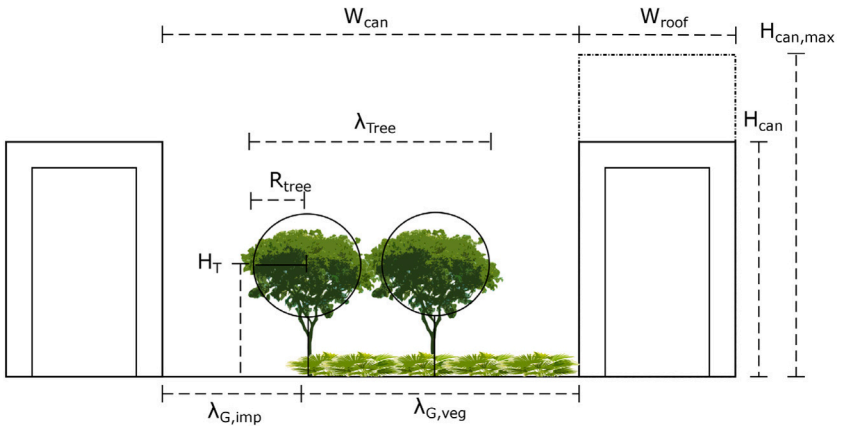


**Fig. 1.** Specification of urban geometry, vegetation cover, and structure in UT&C based on an infinite urban canyon parameterization. $W_{can}$ refers to the average canyon width, $W_{roof}$ to the average roof width, $H_{can}$ to the average canyon height, and $H_{can,max}$ to the maximum building height observed in the neighbourhood. Vegetation fractions are specified by $\lambda_{Tree}$ and $\lambda_{G,veg}$, which are the plan area fraction of tree and vegetated ground cover within the canyon, respectively. $H_T$ refers to the tree height, $R_{tree}$ to the tree radius, which is one fourth of $\lambda_{Tree}$. $\lambda_{G,imp}$ refers to the impervious ground fraction within the canyon.

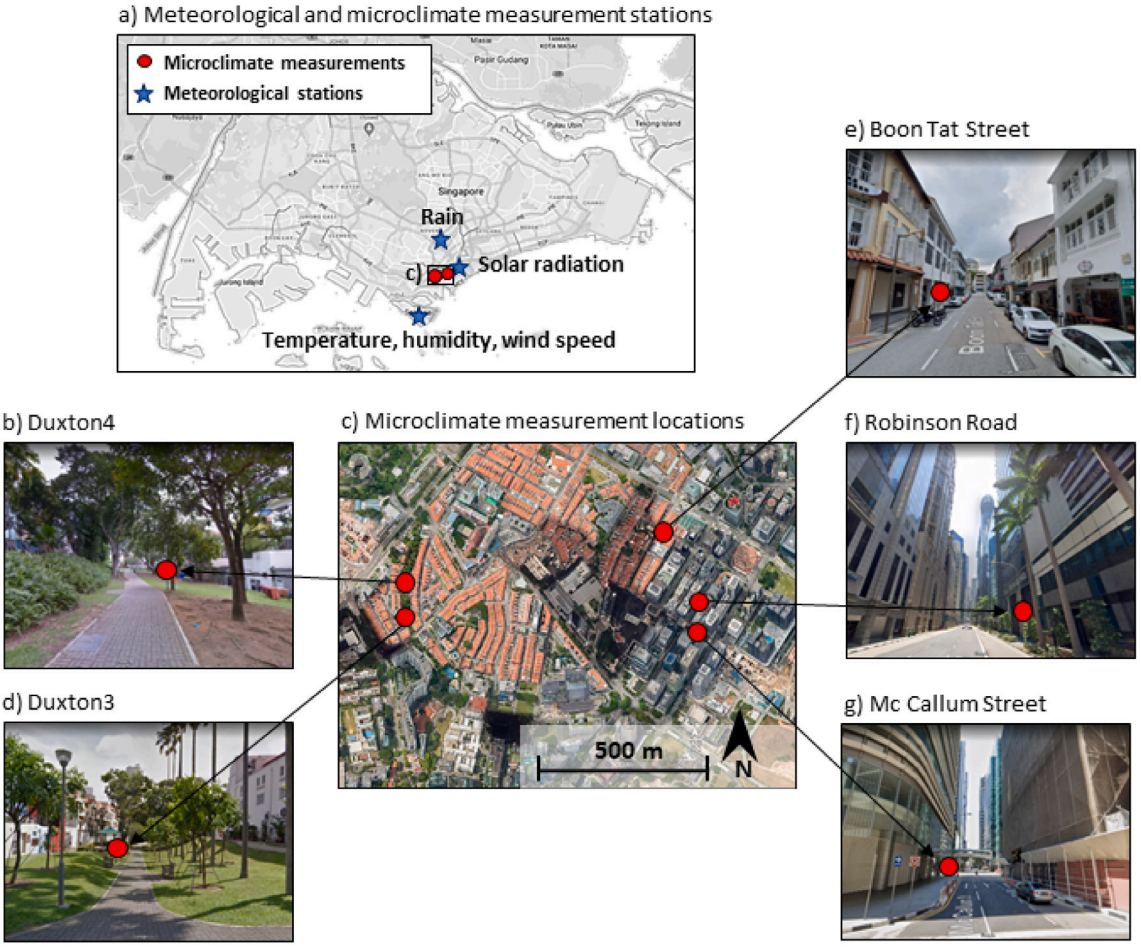


**Fig. 2.** Measurement locations of the data used as meteorological forcing to the model (temperature, humidity, wind speed, solar radiation, and rain) and locally observed microclimate variables ($T_{2m}$, $RH_{2m}$, $WS_{2m}$, and $T_{mrt}$). (a) Overview of measurement locations in Singapore, (c) Overview of the microclimate measurement locations in (b) Duxton4, (d) Duxton3, (e) Boon Tat Street, (f) Robinson Road, and (g) Mc Callum Street. Red points indicate the lamp posts on which the measurement equipment was mounted on. Pictures are from Google maps [43].

high fraction of grass covering the ground, young tree cover, as well as tall palm trees, and (3) Duxton4 with a high ground vegetation fraction as well as mature tree canopies covering the measurement site. Furthermore, two of the microclimate stations were set-up in perpendicular dense high-rise urban canyons: Robinson Rd. (north-east orientation) with little vegetation cover and Mc Callum St. (north-west orientation) without vegetation in the Central Business District (CBD) of Singapore. The extraction of the landcover fractions, urban form, and vegetation physical properties surrounding the measurement locations is described in Section 2.2.2.

Measurement duration was approximately four months (4th of July 2019 – 11th of November 2019) for Duxton3 and Duxton4, five months (15th of November 2019 – 18th of April 2020) for Boon Tat St., six months (25th of October 2019 – 18th of April 2020) for Robinson Rd., and only two months for Mc Callum St. (15th of November 2019 – 13th of January 2020) due to damage of the instruments. Note, that the measurement periods differ for the locations in Duxton versus CBD, so that concurrent differences cannot be computed.

Two devices were used to measure the required climate variables: (1) The passively ventilated Weather Transmitter (WXT520) from Vaisala measured wind speed, air temperature and relative humidity, (2) a black globe radiant temperature sensor (150 mm diameter) from Scientific Campbell measured globe temperature, from which $T_{mrt}$ was derived. The sensors were mounted on a metallic arm extending up to 1.2 m laterally from a lamppost to avoid any wind obstructions from the post. The sensors in Duxton3 and Duxton4 were mounted at a height of 2.2 m while in the other locations the sensors were mounted at a height of 2.4 m due to requirements aiming to avoid interference with pedestrians and vehicles. 1-min records were stored in a datalogger (Scientific Campbell CR300). From these, 1-h mean climatic values were calculated and used for the model performance assessment.

UT&C requires incoming short ($S\downarrow$) and longwave ($L\downarrow$) radiation, precipitation ($Pr$), air temperature ($T_{atm}$), humidity ($RH_{atm}$), and wind speed ($Ws$) at forcing height (typically above the city canyon) as meteorological input to the model specifying the local weather conditions. The meteorological forcing data ($T_{atm}$, $RH_{atm}$, $Ws$, $Pr$), is obtained from the meteorological network of the National Environment Agency (NEA) of Singapore. Station selection is based on proximity to the microclimate measurement locations and continuous data availability. Measurement height of $T_{atm}$, $RH_{atm}$, and $Ws$ is at 37 m. The incoming direct and diffuse solar radiation data was acquired from the Solar Energy Research Institute of Singapore (SERIS). Incoming longwave radiation was calculated using a weather generator [44]. The location of the meteorological and radiation stations in relation to the micro climate measurement location is displayed in Fig. 2 and the time series of the meteorological forcing data ($S\downarrow$, $L\downarrow$, $T_{atm}$, $RH_{atm}$, $Ws$, $Pr$) is displayed in Fig. B.1. The whole data time series to force the model spans from 1st of July 2019 to 1st of May 2020 at hourly resolution.

#### 2.2.2. Model set-up: Urban geometry

UT&C requires specification of parameters describing urban and vegetation geometry and properties. The average urban form and composition, such as $H_{can}$, $H_T$, $\lambda_{Tree}$, $\lambda_{G,veg}$, $\lambda_{G,imp}$, and plan area fraction of buildings surrounding each measurement location was extracted from a landcover, building and tree height map [33] within a radius of 150 m. $W_{roof}$, $W_{can}$, and $R_{tree}$ were calculated based on the landcover plan area fractions and under the assumption that the total tree cover is present within the urban canyon.

The 5 measurement locations are within and around Singapore's CBD, which is highly heterogenous with patches of low and high-rise urban areas next to each other. The presence of high-rise buildings next to low-rise areas can affect the heat and water vapour convection efficiency through the interaction with the wind flow above the buildings and the enhancement of turbulence (Fig. B.3). While a radius of 150 m from the measurement points provided a fairly homogeneous urban form as required by UT&C's radiation parameterization, a radius of 300 m was chosen to extract the $H_{can,std}$ and $H_{can,max}$ for the calculation of urban roughness and displacement height [35] to account for the influence of the observed urban heterogeneity on the turbulent energy exchange. In homogeneous urban areas such a variation of the extraction radii would not be necessary, as roughness properties would also be homogenous [e.g.27].

The high vegetation and tree cover amount at measurement locations Duxton3 and Duxton4 is not representative of this neighbourhood but unique to a backlane rebuilt as a park within an urban canyon. Hence, the ground vegetation and tree fractions calculated within a 150 m radius from locations Duxton3 and Duxton4 is considerably lower than the vegetation cover directly surrounding the sensor. Especially $T_{mrt}$ and $Ws_{2m}$ can be heavily influenced by the presence or absence of trees in the direct proximity, as trees cast shade as well as alter the wind flow. To analyse this effect, model simulations were also performed with the average vegetation cover amount directly surrounding the sensors within a radius of 15 m.

Furthermore, the measurement location in Boon Tat Street is located in close proximity to high-rise buildings, which can cast shade onto Boon Tat Street. Hence, the shade at street level, used in the computation of $T_{mrt}$ in Boon Tat Street, is calculated using the radiation terrain algorithm of T&C [30,45] and a digital surface model of the area [33].

The extracted urban form and vegetation cover for each of the five measurement locations used in the model performance assessment are summarized in Table B.1. Anthropogenic heat input was based on literature [46] and depends on urban density and use. Furthermore, the parameters specifying urban and vegetation properties were assigned based on literature and expert knowledge. These values are summarized in Table 1 (specified as "Default value SG" in which SG denotes "Singapore") and Table B.3.

#### 2.2.3. Model performance assessment

Model simulations were compared against microclimate measurements of $T_{2m}$ [°C], $RH_{2m}$ [%], $Ws_{2m}$ [m s$^{-1}$], and $T_{mrt}$ [°C], as well as their aggregation into the OTC index UTCI [14,15], to assess model performance. Note, that wind speed was measured at 2.2 and 2.4 m (in different locations) height, but UTCI requires a wind speed input at a height of 10 m. Hence, measured wind speed was back-computed to 10 m height using the wind profile calculated in UT&C, which applies a logarithmic wind profile above the urban canyon and an exponential wind profile within the urban canyon [27].

Model performance assessment is based on the coefficient of determination ($R^2$), total, systematic, and unsystematic root mean square error ($RMSE$, $RMSE_{sys}$, $RMSE_{unsys}$), mean bias error ($MBE$), and mean absolute error ($MAE$) [47], which were calculated including the full measurement time period at hourly time steps. Furthermore, the simulated and measured average diurnal cycles of the microclimate variables and UTCI were compared.

### 2.3. Sensitivity analysis

UT&C includes a large set of parameters, that specify vegetation amount, structure, optical properties, canopy interception, and plant physiology. All these parameters influence the model output, but accurate parameter values can be difficult to estimate due to limited data as well as naturally occurring variability and heterogeneity within the urban environment and within vegetation. We perform a sensitivity analysis of UT&C's vegetation parameters that can (a) quantify the uncertainty in model output due to uncertainty in vegetation input parameters (Section 2.3.2), hence, (b) pin-point important parameters, which need to be assigned carefully (Section 2.3.3 and Section 2.3.4), and (c) quantify the overall expected effect of a change in urban vegetation cover on UTCI in Singapore (Section 2.4). The variance based sensitivity analysis is performed in four different urban densities as specified in Section 2.3.1.

The model structure of UT&C is complex with non-linear interactions between parameters. Hence, the model is treated as a black-box in the performed sensitivity analysis without any assumption on parameter interactions. The sensitivity analysis is focused on OTC represented with UTCI and its contributing meteorological variables ($T_{2m}$, $RH_{2m}$, $Ws_{10m}$, and $T_{mrt}$).

#### 2.3.1. Specification of urban form for the variance based sensitivity analysis

The vegetation parameter sensitivity analysis is performed in four urban densities, which are defined according to representative values of local climate zones LCZ 2 (compact midrise), LCZ 3 (compact lowrise), LCZ 5 (open midrise), and LCZ 6 (open lowrise) as defined by [48]. The canyon aspect ratio $H_{can}/W_{can}$ is equal to the average aspect ratio defined by [48] for each analysed LCZ, $H_{can}$ is equal to the average height of roughness elements, $H_{can,max}$ is equal to the maximum height of roughness elements, and $H_{can,std}$ is assumed to be 1/4 of the range of height of roughness elements for each analysed LCZ as specified by [48]. $W_{can}$ was calculated based on the ratio of $H_{can}/W_{can}$. $W_{roof}$ was calculated based on the average building plan area fraction specified by [48] and $W_{can}$. The vegetation fraction is allowed to vary in the analysed LCZs as it is the focus of this study. A priori, the vegetation parameter effects on UTCI are expected to be different between urban densities, for example, due to varying sunlight availability for plant photosynthesis or convection efficiency. The urban geometry of the four analysed urban densities (LCZ2, LCZ3, LCZ5, and LCZ6) is defined in Table B.2. Note, that the four analysed LCZ scenarios in the sensitivity analysis do not correspond to the exact urban density and land cover around the micro climate measurement stations used for model performance assessment but are four hypothetical scenarios. UT&C also includes a range of parameters that specify material properties. These parameters are assigned to standard values as summarized in Table B.3.

#### 2.3.2. Parameter selection and range

A total of 25 vegetation parameters were selected for the sensitivity analysis (Table 1). These parameters can be grouped in five broad categories that specify: (1) vegetation amount, (2) physical structure, (3) optical properties, (4) rainfall interception, and (5) physiology of trees and ground vegetation.

For sake of generality, the parameter range (Table 1) is determined according to parameter values representing global observations, as plant properties vary widely also within the same climate and non-native species are common in Singapore's urban greenery [49–52]. Such a global parameter range quantifies the maximum expected effect of vegetation on UTCI. Model parameters are considered independent random variables and their occurrence over the parameter spaces is defined by either a uniform or a symmetric Beta distribution. The parameters of the Beta distribution were selected such that ± 3 standard deviations cover the full parameter space. A Beta distribution is chosen for parameters where extreme values are representative of rare plant species and are less likely to occur. This reduces the overestimation of model sensitivity and uncertainty caused by unrealistic parameter combinations.

Model simulations for the subsequent analyses (Sections 2.3.3 to 2.5) were performed over a time period of 10 months (July 2019 to May 2020) using the forcing data described in Section 2.2.1 and shown in Fig. B.1. Vegetation is assumed to be fully irrigated through drip irrigation to exclude any effect of water stress in the analysis. While water stress could be important when analysing vegetation effects on urban climate, it represents an unusual condition for Singapore's climate and is not the focus of this study.

It is important to note that in this study the mean radiant temperature is calculated at a point 1 m from the tree trunk at a height of 2 m if the tree height and crown area permit. In the case of shorter trees, the point is placed 0.5 m from the tree crown at 2 m height. Such a placement assumes that people would walk underneath tree cover if possible and hence, the average $T_{mrt}$ exposure, includes both sun and shade, depending on the time of the day and year.

#### 2.3.3. Parameter screening: Elementary effects

A full variance based sensitivity analysis with many parameters is computationally expensive as a large number of model evaluations are needed to reach sensitivity index convergence [65]. Under the assumption that UT&C has a few influential parameters and many non-influential ones, a computationally less expensive screening sensitivity analysis can be performed [31,66], such as the method of elementary effects (EE) [31,65,67].

This method uses individually randomized one-at-a-time designs that cover a wide range of variations over the entire parameter space. The absolute mean ($\mu_{|EE|}$) and the standard deviation ($\sigma_{EE}$) of the derivatives, called elementary effects ($EE_i$), are used to rank the relative parameter importance [31,65,67]. $EE_i$ is calculated as follows, defining $Y = f(X)$ as a generalized model output and $X = X_1, \ldots, X_k$ as the vector of k probabilistically distributed parameters [65,67]:

$$EE_i = \frac{Y(x_1, \ldots, x_i + \Delta, \ldots, x_k) - Y(x_1, \ldots, x_k)}{\Delta}, \tag{3}$$

where $\Delta$ is the parameter variation magnitude, and $x_1, \ldots, x_k$ are the realizations of $X_1, \ldots, X_k$. The mean of the elementary effect ($\mu_{|EE|}$) is an estimator of the total parameter influence on the output variable, while the standard deviation ($\sigma_{EE}$) indicates higher-order effects. In the presented study, the Euclidian distance of $(\mu_{|EE|}, \sigma_{EE})$ from the origin (0,0), $\epsilon = \sqrt{\mu_{|EE|}^2 + \sigma_{EE}^2}$, is used for the overall parameter ranking [31]. The computational protocol of the method of EE is described in detail in [67].

The EE screening test is performed for all four urban densities (LCZ2, LCZ3, LCZ5, LCZ6) to qualitatively assess the relative importance of each of the 25 parameters (Table 1). As model outputs are time series, the mean of the output variable over the total simulation period (10 months at hourly time steps) is used to perform the EE screening. Parameter importance is determined according to whether a parameter ranks in the top 10 $\epsilon_i$ for any of the analysed LCZs. The EE method output is qualitative and parameters are ranked in terms of relative importance without information on how much more important a given parameter is compared to the others or how parameters interact [31,66]. Hence, a variance based sensitivity analysis is subsequently performed (Section 2.3.4) to quantitatively assess the individual parameter importance.

#### 2.3.4. Variance based sensitivity analysis

The subset of most important parameters identified through the EE screening method (Section 2.3.3) is further analysed through a variance-based sensitivity analysis following the Sobol methodology [31,68–70]. The Sobol sensitivity analysis is based on a functional analysis of variance (ANOVA) [71] under the assumption that model uncertainty is fully captured by its output variance [31].

Model response Y of a generalized model $Y = f(\mathbf{X})$ with a total number of k probabilistically distributed parameters specified in vector $\mathbf{X} = \{X_1, \ldots, X_k\}$ is partitioned into summands of increasing dimensionality according to the criteria specified by [68]. The decomposition is then squared and integrated to partition the output variance, $V_Y$, into terms of increasing dimensionality as:

$$V_Y = V[Y] = V[f(\mathbf{X})] = \sum_{i}^{k} V_i + \sum_{i=1}^{k}\sum_{j>i}^{k} V_{ij} + \cdots + V_{1\ldots k} \tag{4}$$

where $V_i = V\left[E\left[Y \mid X_i = x_i^*\right]\right]$, and $V_{ij} = V\left[E\left[Y \mid X_i = x_i^*, X_j = x_j^*\right]\right] - V_i - V_j$. $E[\cdot|\cdot]$ denotes the conditional expectation, and $x_i^*, x_j^*$ are the respective real values of parameter i and j. Subsequently, the sensitivity indices are calculated as the ratio of partial variance caused by parameter i to the overall output variance:

$$1 = \sum_{i}^{k} S_i + \sum_{i=1}^{k}\sum_{j>i}^{k} S_{ij} + \cdots + S_{1\ldots k} \tag{5}$$

where $S_i$ is the main effect of parameter i (first order sensitivity index), while $S_{ij}$ represents the interactions of parameter i and j (second order sensitivity index).

In this study, the total order sensitivity index $S_{Ti}$ is analysed, which includes the main effects as well as all interaction effects of

**Table 1**
Vegetation parameter ranges and distribution for the elementary effects (EE) prescreening and the variance based sensitivity analysis. Singular vegetation parameters used for the model comparison simulations (Default value SG) are also reported. In performing the EE prescreening, all listed vegetation parameters vary across the specified ranges. In performing the variance based sensitivity analysis, only the vegetation parameters with parameter ranges marked in bold vary, while the remaining vegetation parameters are set at the default value for Singapore. For the model comparison simulations, all vegetation parameters are set at the default value for Singapore unless otherwise specified in the table. Parameter range selection is based on literature values, or approximated based on expert judgement.

| Parameter | Description | Parameter range | Sample distribution | Default value SG | Reference |
|---|---|---|---|---|---|
| **Vegetation amount** | | | | | |
| $\lambda_{Tree}$ | Tree cover within canyon (–) | **0.05–0.95** | Uniform | site specific | |
| $\lambda_{G,veg}$ | Vegetated ground fraction within canyon (–) | **0–1** | Uniform | site specific | |
| $LAI_T$ | Tree leaf area index (–) | **0.5–6.5** | Beta | 3 | [53,54] |
| $LAI_G$ | Ground vegetation leaf area index (–) | **0.5–6.5** | Beta | 2.5 | [53] |
| **Vegetation structure** | | | | | |
| $H_T$ | Tree height (m) | **3 - $H_{can}$** | Beta | site specific | [55] |
| $d_T$ | Distance of tree trunk from wall within available space (–) | **0.05–0.95** | Uniform | site specific | |
| $hc_G$ | Canopy height of ground vegetation (m) | **0.02–0.15** | Uniform | 0.05 | |
| $d_{leaf,T}$ | Tree leaf dimension (cm) | **1–10** | Uniform | 5 | [56] |
| $d_{leaf,G}$ | Ground vegetation leaf dimension (cm) | 0.5–3 | Uniform | **2** | [56] |
| $K_{opt,T}$ | Tree canopy light extinction coefficient (–) | **0.38–0.70** | Beta | 0.5 | [57] |
| $K_{opt,G}$ | Ground vegetation canopy light extinction coefficient (–) | 0.22–0.74 | Beta | **0.5** | [57] |
| **Optical properties** | | | | | |
| $\alpha_T$ | Albedo of tree (–) | 0.15–0.25 | Beta | **0.27** | [58,59] |
| $\alpha_G$ | Albedo of vegetated ground (–) | 0.18–0.3 | Beta | **0.27** | [58,59] |
| **Canopy interception parameters** | | | | | |
| $S_{P,In,G}$ | Specific water retained by ground vegetation surface (mm $m^2$ PFT area $m^{-2}$ leaf area) | 0.1–0.4 | Beta | **0.2** | [60,61] |
| $S_{P,In,T}$ | Specific water retained by tree surface (mm $m^2$ PFT area $m^{-2}$ leaf area) | 0.1–0.4 | Beta | **0.1** | [60,61] |
| **Physiological parameters** | | | | | |
| **Trees** | | | | | |
| $\Delta_{0,T}$ | Empirical coefficient that expresses the value of vapour pressure deficit at which $f(\Delta e) = 0.5$ (Pa) | **800–2500** | Beta | 2000 | [62] |
| $a_{1,T}$ | Empirical parameter linking net assimilation $A_{nC}$ to stomatal conductance $g_{s,CO_2}$ (–) | **5–10** | Beta | 9 | [62] |
| $K_{N,T}$ | Canopy nitrogen decay coefficient (–) | 0.2–0.5 | Beta | **0.5** | |
| $V_{c,max,T}$ | Maximum Rubisco capacity at 25 °C leaf scale (μmol $CO_2$ $m^2$s) | **20–100** | Beta | 49 | [27,63,64] |
| $S_{LAI,T}$ | Specific leaf area ($m^2$ LAI $gC^{-1}$) | 0.012–0.032 | Beta | **0.02** | |
| **Ground vegetation** | | | | | |
| $\Delta_{0,G}$ | Empirical coefficient that expresses the value of vapour pressure deficit at which $f(\Delta e) = 0.5$ (Pa) | 800–2500 | Beta | **2000** | [62] |
| $a_{1,G}$ | Empirical parameter linking net assimilation $A_{nC}$ to stomatal conductance $g_{s,CO_2}$ (–) (C4 grass) | 3–5 | Beta | **5** | [62] |
| $K_{N,G}$ | Canopy nitrogen decay coefficient (–) | 0.1–0.4 | Beta | **0.3** | |
| $V_{c,max,G}$ | Maximum Rubisco capacity at 25 °C leaf scale (μmol $CO_2$ $m^2$s) | 20–100 | Beta | **54** | [27,63,64] |
| $S_{LAI,G}$ | Specific leaf area ($m^2$ LAI $gC^{-1}$) | 0.015–0.045 | Beta | **0.025** | |

the parameter of interest. $S_{Ti}$ gives a robust estimation of parameter importance and interactions [72,73]. For independent parameters (orthogonal case), $S_{Ti}$ can be calculated as the sum of all terms of Eq. (5) that include parameter i [66], and is defined as:

$$S_{Ti} = \frac{E\left[V\left[Y \mid \mathbf{X}_{\sim i}\right]\right]}{V[Y]} = 1 - \frac{V\left[E\left[Y \mid \mathbf{X}_{\sim i}\right]\right]}{V[Y]} \quad (6)$$

where $\mathbf{X}_{\sim i}$ is a vector of all probabilistically distributed parameters except the $i$th. There are multiple computational methods to calculate $E\left[V\left[Y \mid \mathbf{X}_{\sim i}\right]\right]$ [72,74,75], and we follow the approach of [74]. Further information and the detailed computational protocol of Sobol's sensitivity analysis [68] can be found in [31,69,70]. The Sobol low discrepancy sequence [76,77] is chosen as sampling strategy due to its enhanced convergence rate of the numerically estimated sensitivity indices [69]. A convergence test was conducted to define the necessary number of model runs. A total of 14,336 model evaluations per LCZ were selected. Uncertainty bars of the sensitivity indices were calculated using bootstrapping [71] with 1000 bootstrap replicates.

As model outputs are time series, the mean of the output variables including the entire 10 months (all weather conditions) is used to calculated $S_{Ti}$ for four different time periods of the day. The four groups were night (1900–0700 local time, LT), morning (0800–1100 LT), midday (1200–1400 LT), and afternoon (1500–1800 LT). In Singapore, there is minimal difference in daylight length throughout the year and solar noon is around 1300 LT.

### *2.4. Influence of vegetation amount and properties on diurnal outdoor thermal comfort*

The influence of vegetated ground and tree cover plan area fraction within the urban canyon, $\lambda_{G,veg}$ and $\lambda_{Tree}$ (Fig. 1), as well as of the remaining vegetation parameters on UTCI is analysed for the four different urban densities (LCZ 2, 3, 5, and 6, Section 2.3.1) and the four different time periods using the 14,336 model evaluations necessary for the variance based sensitivity analysis (Section 2.3.4). The results are analysed as follows:

1. The hourly simulation outputs of each time series and for each model evaluation are binned according to the time periods i.e., portions of the day as specified above (Section 2.3.4) using the entire 10 months time series with all occurring weather conditions.
2. These binned time series are averaged for each model evaluation within each time bin.

3. For each combination of $\lambda_{G,veg}$ and $\lambda_{Tree}$:

   (a) the average UTCI is calculated including all model evaluations.
   (b) the difference between the 95th and 5th percentiles of UTCI in the different model evaluations is calculated.

The result of step 3a represents the average expected UTCI, if only ground vegetation and tree fractions are specified but vegetation properties are allowed to vary. For example, in a defined urban density at 30% grass and 20% tree cover plan area fraction within the urban canyon, the UTCI is expected to be x°C on average if there is no accurate assignment of tree height, leaf area index, or tree photosynthetic properties. The result of step 3b represents the range of variability (5th–95th percentile) expected for UTCI that can be achieved through a change in vegetation properties for a given combination of $\lambda_{G,veg}$ and $\lambda_{Tree}$. For example, in a defined urban density with 30% grass and 20% tree cover plan area fraction within the urban canyon, it represents how much UTCI could be modified if plant parameters were changed according to the above specified ranges, which leads to a best and worse OTC for a given configuration of vegetation fractions.

The effect of humidity increase on UTCI due to vegetation is further analysed through the removal of variability of humidity with $\lambda_{G,veg}$ and $\lambda_{Tree}$. This means that UTCI is also calculated with the average simulated humidity in the vegetation fraction combination bin of $0 < \lambda_{G,veg} < 0.05$ and $0.05 < \lambda_{Tree} < 0.1$ (Figure C.11).

### 2.5. Vegetation properties that enhance thermal comfort during periods of extreme heat

Urban vegetation should not only improve climatic conditions on average, but it should do so especially during heat waves. Hence, the distribution of vegetation parameters, which provide the lowest UTCI during the 5% hottest hours of the years is also analysed. For this purpose, we first determine the 95% percentile of UTCI for each model evaluation time series. Subsequently, the 10% model evaluations with the lowest 95% percentile of UTCI are selected. For these 10% "coolest" model evaluations, histograms of parameter distributions are plotted, which identify parameter selections that result in higher cooling during peak temperatures. Note, the histograms would show a uniform distribution if all or a random selection of model evaluations were included as this is the set-up of the sensitivity analysis. For the parameters which follow a Beta distribution, the displayed parameter distribution in the results section is back-transformed to also follow a uniform distribution if all model evaluations were included.

## 3. Results

### 3.1. Model performance assessment

The model and measurements comparison (Fig. 3, Table 2) shows a relatively good agreement considering any lack of model calibration between simulated and measured $T_{2m}$, $RH_{2m}$, $T_{mrt}$, and UTCI in low to mid-rise settings such as Boon Tat St., Duxton3, and Duxton4. However, this is true only if the high tree cover, surrounding the measurement location at Duxton4, is included in the calculation of $T_{mrt}$ and UTCI, otherwise, $T_{mrt}$ and UTCI are over-predicted in Duxton4 due to the lack of tree shade as illustrated in Fig. 3q and v (blue vs red lines).

High $R^2$ values are observed for $T_{2m}$ with 0.82, 0.79, and 0.81 and $RH_{2m}$ with 0.86, 0.82, and 0.86 for Duxton3, Duxton4, and Boon Tat St., respectively. The RMSE for the same sites is 1.2 °C, 1.4 °C, and 1.2 °C, and 6.7 %, 6.7 %, and 7.0 % for $T_{2m}$ and $RH_{2m}$, respectively. There is a very likely constant offset between the humidity measurements, which are used as model forcing data, and the real relative humidity above the microclimate measurements leading to a consistent over-prediction of $RH_{2m}$. This offset is most clearly shown at night (Fig. B.2). Additional discrepancies might be due to the fact, that UT&C is likely underestimating daytime convection efficiency for the turbulent transport of heat and water vapour, which leads to a slight overestimation of the $T_{2m}$ mean diurnal cycle amplitude as can be seen in Fig. 3.

High $R^2$ values are also observed for $T_{mrt}$ in Duxton3 and Duxton4 with 0.80 and 0.81, while $R^2$ is lower for Boon Tat St. with 0.59. Boon Tat St. has a higher unsystematic than systematic RMSE (5.2°C vs 0.8°C) indicating that most of the error is likely introduced by a process that cannot be reproduced by the model. $T_{mrt}$ is highly influenced by the presence or absence of direct solar radiation. During the measurement period at Duxton3 and Duxton4 (July 2019 to mid November 2019) incoming solar radiation is high and rainfall scarce, while during the measurement period at Boon Tat St. (mid November 2019 to mid April 2020) incoming direct solar radiation decreases and rain occurs more often (Fig. B.1). Such a shift in meteorological conditions likely emphasizes the slight mismatch between the meteorological conditions at the location where model forcing data was measured and the actual meteorological conditions directly above the micro climate stations and decreases the modelled $R^2$ for $T_{mrt}$ as rainfall and cloud cover are highly localized in Singapore. The RMSE for $T_{mrt}$ is 6.5 °C, 7.2 °C, and 5.3 °C for Duxton3, Duxton4, and Boon Tat St., respectively.

Similar to $T_{mrt}$, UTCI shows high $R^2$ values for Duxton3 and Duxton4 with 0.84 and 0.81, and a lower $R^2$ for Boon Tat St. with 0.70 which is likely caused by the effects of $T_{mrt}$. The RMSE for $UTCI$ is 2.0 °C, 2.8 °C, and 1.9 °C for Duxton3, Duxton4, and Boon Tat St., respectively.

In dense high-rise settings, such as McCallum St. and Robertson road, $T_{2m}$, $T_{mrt}$, and UTCI are overestimated by the model simulations during daytime (Fig. 3). This overestimation is possibly caused by the integrated radiation scheme of UT&C, which overpredicts surface temperatures at pedestrian level in dense high-rise settings, as the absorbed radiation by a partly sunlit wall is averaged over the total wall area. Such a higher surface temperature also leads to higher $T_{mrt}$ and possibly higher $T_{2m}$ as seen in Fig. 3s, t, d, and e. As the general trends of UTCI in dense high-rise settings are not properly reproduced by UT&C as shown here, the sensitivity analysis (Sections 3.2 to 3.5) will only focus on low and mid-rise urban areas.

As shown by the low $R^2$ values (Table 2), wind speed is not well predicted by UT&C in any of the analysed scenarios. However, the average magnitude is correctly reproduced for medium to low rise settings. The lack of temporal correlation between observed and simulated wind speed was expected, as wind speed is highly influenced by the detailed urban geometry while UT&C applies a general wind profile parameterization calculated based on the observed average urban fabric.

In summary, UT&C's parameterization is based on the neighbourhood scale, which is likely also the spatial scale that determines the measured $T_{2m}$ and $RH_{2m}$ due to turbulent mixing of air, while $T_{mrt}$ and $Ws_{2m}$ are highly influenced by the local geometry which can cast shade or block wind-flow at the specific point of observation. Hence, while UT&C predicts $T_{2m}$ and $RH_{2m}$ well using the average neighbourhood landcover fraction (radius 150 m), it performs better for $T_{mrt}$ when using the landcover composition of the immediate sensor environment (radius 15 m), as seen by the example of Duxton4. In the subsequent sensitivity analysis, it is assumed that the low- to mid-rise urban settings (LCZ2, LCZ3, LCZ5, and LCZ6) are homogeneous neighbourhoods to align the scales of $T_{2m}$, $RH_{2m}$, $T_{mrt}$, $Ws_{2m}$, and UTCI.

### 3.2. Elementary effects

The performed EE pre-screening of 25 selected vegetation parameters identifies vegetation amount, structure, and tree physiological parameters as the most influential on UTCI in Singapore (Fig. 4). The parameters specifying plant interception, albedo, and ground vegetation physiology influence UTCI to a lesser extent. This is largely due to the amount of photosynthetic active radiation available to both vegetation types (ground vegetation and trees). Ground vegetation is more often shaded by buildings and tree canopies than trees themselves

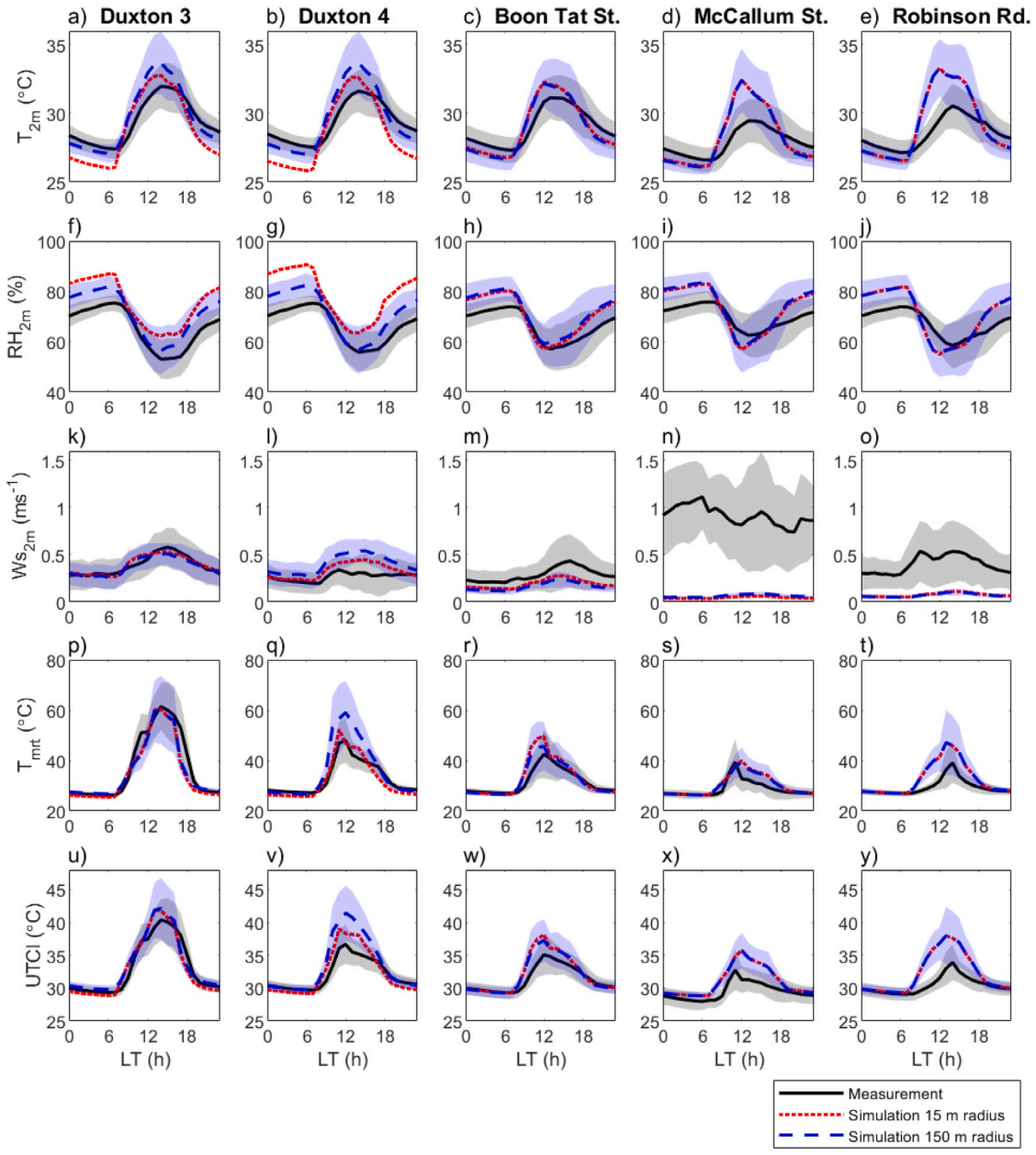


**Fig. 3.** Model performance assessment through the comparison of mean diurnal cycles ± 1 standard deviation of measured and simulated $T_{2m}$, $RH_{2m}$, $Ws_{2m}$, $T_{mrt}$, and UTCI for the measurement locations of (a) Duxton3, (b) Duxton4, (c) Boon Tat St., (d) McCallum St., (e) Robinson Rd using the whole simulation period for each location. Red lines depict the simulated mean diurnal cycle obtained with simulations using the vegetation cover fractions within a 15 m radius of the microclimate sensors rather than 150 m. (For interpretation of the references to colour in this figure legend, the reader is referred to the web version of this article.)

and hence, receives on average less solar radiation to perform photosynthesis. Therefore, the physiological parameters governing ground vegetation response become less important.

As parameter sensitivity can depend on time of the day, the Euclidean distance ($\epsilon_i$) was also analysed for day and night time separately in each urban density (not shown). Although, the relative ranking of the top 10 parameters varied between day and night time, this did not translate into a different selection of the most important parameters. Furthermore, there are no clear differences in the results of the EE pre-screening between the analysed LCZs (Fig. 4).

The EE pre-screening lead to a selection of a total of 12 parameters used in the variance based sensitivity analysis: vegetation parameters defining vegetation amount ($\lambda_{Tree}$, $\lambda_{G,veg}$, $LAI_T$, $LAI_G$), vegetation structure ($H_T$, $d_T$, $d_{leaf,T}$, $K_{opt,T}$, $h_{c,G}$), as well as tree physiology ($V_{c,max,T}$, $a_{1,T}$, $\Delta_{0,T}$) were selected. The remaining parameters were set at their default value (Table 1). The selected parameter ranges and values for the full variance based sensitivity analysis are marked in bold in Table 1.

### 3.3. Variance based sensitivity analysis

UTCI is influenced by ground vegetation, $\lambda_{G,veg}$, and tree cover fraction, $\lambda_{Tree}$, but also by the tree height and placement (Fig. 5a). The effects of $\lambda_{Tree}$ and $\lambda_{G,veg}$ differ during day and night time. During daytime, $\lambda_{Tree}$ has a higher influence on UTCI than $\lambda_{G,veg}$, while the opposite is true during night time, a trend also shown in Section 3.4. Furthermore, during midday and afternoon, the parameter maximum Rubisco capacity, $V_{c,max,T}$, governing photosynthesis, as well as LAI and optical density of the tree canopy, $K_{opt,T}$, also affect UTCI, but to a lesser extent than the other parameters.

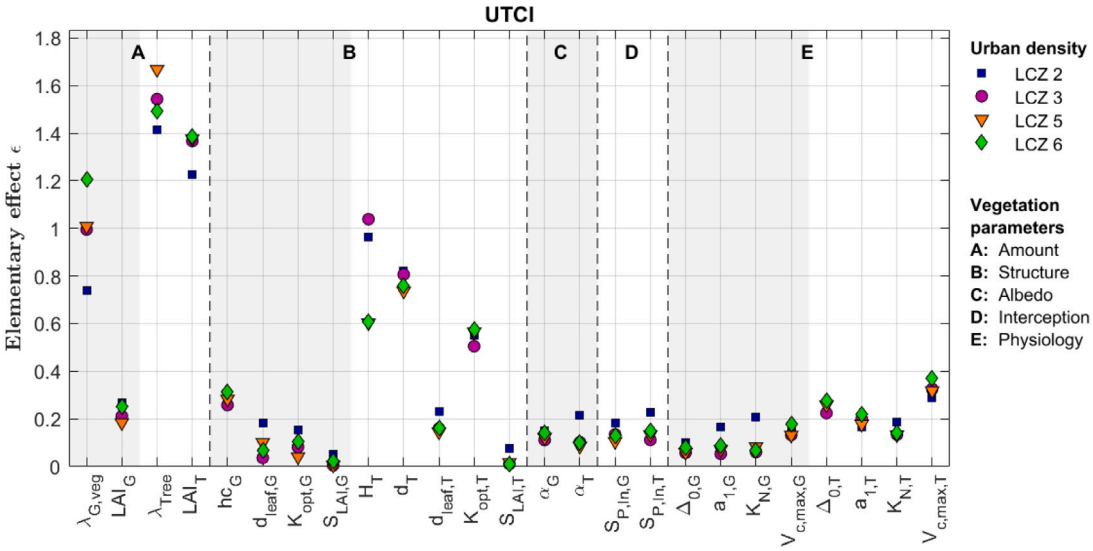


**Fig. 4.** Total elementary effect $\epsilon$ of the 25 vegetation parameters specified in Table 1 on UTCI for LCZ 2, 3, 5, and 6.

**Table 2**
Coefficient of determination ($R^2$), root mean square error (RMSE), systematic root mean square error ($RMSE_{sys}$), unsystematic root mean square error ($RMSE_{unsys}$), mean bias error (MBE), and mean absolute error (MAE) of the UT&C model performance assessment against microclimate measurements in 5 locations in downtown Singapore. Model simulations were performed using the vegetation cover fractions within a 150 m radius of the microclimate sensors.

| | $R^2$ | RMSE | $RMSE_{sys}$ | $RMSE_{unsys}$ | MBE | MAE |
|---|---|---|---|---|---|---|
| | (–) | (°C) | (°C) | (°C) | (°C) | (°C) |
| $UTCI$ (Duxton3) | 0.84 | 2.0 | 0.5 | 1.9 | 0.5 | 1.3 |
| $UTCI$ (Duxton4) | 0.81 | 2.8 | 2.0 | 2.0 | 1.4 | 1.7 |
| $UTCI$ (Boon Tat St.) | 0.70 | 1.9 | 0.6 | 1.8 | 0.5 | 1.1 |
| $UTCI$ (McCallum St.) | 0.56 | 2.2 | 1.3 | 1.8 | 1.3 | 1.5 |
| $UTCI$ (Robinson Rd.) | 0.58 | 3.1 | 2 | 2.3 | 1.7 | 1.9 |
| $T_{2m}$ (Duxton3) | 0.82 | 1.2 | 0.5 | 1.1 | 0.2 | 0.9 |
| $T_{2m}$ (Duxton4) | 0.79 | 1.4 | 0.6 | 1.2 | 0.2 | 1.0 |
| $T_{2m}$ (Boon Tat St.) | 0.81 | 1.2 | 0.5 | 1.1 | −0.2 | 1.0 |
| $T_{2m}$ (McCallum St.) | 0.62 | 1.7 | 0.6 | 1.6 | 0.2 | 1.3 |
| $T_{2m}$ (Robinson Rd.) | 0.62 | 2.0 | 1.0 | 1.8 | 0.6 | 1.4 |
| $T_{mrt}$ (Duxton3) | 0.80 | 6.5 | 3.0 | 5.8 | −1.4 | 3.7 |
| $T_{mrt}$ (Duxton4) | 0.81 | 7.2 | 4.7 | 5.4 | 2.8 | 3.9 |
| $T_{mrt}$ (Boon Tat St.) | 0.59 | 5.3 | 0.8 | 5.2 | 0.8 | 2.8 |
| $T_{mrt}$ (McCallum St.) | 0.52 | 3.9 | 1.5 | 3.6 | 1.1 | 2.3 |
| $T_{mrt}$ (Robinson Rd.) | 0.57 | 6.5 | 3.8 | 5.4 | 3.2 | 3.6 |
| | (–) | (%) | (%) | (%) | (%) | (%) |
| $RH_{2m}$ (Duxton3) | 0.86 | 6.7 | 5.4 | 4.0 | 5.4 | 5.8 |
| $RH_{2m}$ (Duxton4) | 0.82 | 6.7 | 4.9 | 4.6 | 4.8 | 5.6 |
| $RH_{2m}$ (Boon Tat St.) | 0.86 | 7.0 | 5.6 | 4.1 | 5.4 | 6.1 |
| $RH_{2m}$ (McCallum St.) | 0.74 | 7.8 | 4.8 | 6.1 | 4.3 | 6.9 |
| $RH_{2m}$ (Robinson Rd.) | 0.74 | 7.7 | 4.2 | 6.4 | 3.1 | 6.7 |
| | (–) | ($ms^{-1}$) | ($ms^{-1}$) | ($ms^{-1}$) | ($ms^{-1}$) | ($ms^{-1}$) |
| $Ws_{2m}$ (Duxton3) | 0.29 | 0.2 | 0.1 | 0.1 | 0.0 | 0.1 |
| $Ws_{2m}$ (Duxton4) | 0.09 | 0.2 | 0.2 | 0.2 | 0.1 | 0.2 |
| $Ws_{2m}$ (Boon Tat St.) | 0.40 | 0.2 | 0.2 | 0.1 | −0.1 | 0.2 |
| $Ws_{2m}$ (McCallum St.) | 0.18 | 1.0 | 1.0 | 0.0 | −0.8 | 0.8 |
| $Ws_{2m}$ (Robinson Rd.) | 0.08 | 0.4 | 0.4 | 0.0 | −0.3 | 0.3 |

UTCI is calculated as a function of $T_{2m}$, $RH_{2m}$, $T_{mrt}$, and $Ws_{10m}$, which all contribute to a different extent and possibly non-linearly. The individual parameter sensitivities of $T_{2m}$, $RH_{2m}$, $T_{mrt}$, and $Ws_{10m}$ differ substantially as seen in Fig. 5a to d. On one hand, $T_{mrt}$ is most influenced by $\lambda_{Tree}$, tree position and tree height during daytime, while $\lambda_{G,veg}$ is dominant during nighttime (Fig. 5d). On the other hand, $T_{2m}$ shows a higher influence of $\lambda_{G,veg}$ during all times of the day, while $\lambda_{Tree}$ is less influential on $T_{2m}$. Interestingly, the influence of maximum tree Rubisco capacity, $V_{c,max,T}$, on $T_{2m}$ during midday is almost as high as the one of $\lambda_{Tree}$. Meaning, tree type can matter almost as much as tree cover fraction for an air temperature reduction during midday at the local scale. Other physiological ($\Delta_{0,T}$, $a_{1,T}$), and structural ($K_{opt,T}$, $H_T$) parameters, and tree LAI also influence $T_{2m}$ during daytime, but their effect is of lower magnitude. $RH_{2m}$ shows similar parameter sensitivity as $T_{2m}$, however, $\lambda_{G,veg}$ and $\lambda_{Tree}$ are almost equally important and no clear differences between day and night time are observed (Fig. 5c).

The effects of trees on the wind speed profile is governed by a few equations with known influence factors [27,35]. These influencing parameters, which define the urban aerodynamic roughness and displacement height are correctly identified in the sensitivity analysis as shown in Fig. 5e. However, as the model performance showed a lower correlation of predicted wind speed with measurements, the results in Fig. 5e should mostly be seen as a proof of the correctness of the sensitivity analysis.

### 3.4. Vegetation amount and properties: Diurnal effects on UTCI

As can be seen in Fig. 6, UTCI with any combination of tree and ground vegetation fractions ($\lambda_{Tree}$, $\lambda_{G,veg}$) exceeds the upper limit of the comfortable UTCI (26 °C) as defined by [14] during all time periods of the day. Hence, any decrease in UTCI is considered positive in the following analysis.

The effects of $\lambda_{Tree}$ and $\lambda_{G,veg}$ vary considerably throughout the day and in different urban densities (Fig. 6). During night time, an increase in $\lambda_{G,veg}$ decreases UTCI, while an increase in $\lambda_{Tree}$ has less effects. Conversely, an increase in $\lambda_{Tree}$ reduces UTCI more efficiently during daytime, while a change in $\lambda_{G,veg}$ provides less improvement to thermal comfort.

However, there are considerable differences in tree cooling effects across the analysed urban densities during daytime. The open midrise (LCZ 5) as well as the compact low-rise (LCZ 3) typology show a clear decrease in UTCI as $\lambda_{Tree}$ increases during mornings, middays, as well as in the afternoon (Fig. 6f to h and j to l), while the compact midrise (LCZ 2) as well as the open low-rise (LCZ 6) show mixed effects. The open low-rise (LCZ 6) experiences the lowest average UTCI between 30 to 50 % tree cover, depending on time of the day, while a $\lambda_{Tree}$ larger than 50 % of the canyon area, leads to a slightly higher UTCI (Fig. 6n to p). Hence, there seems to be an optimal $\lambda_{Tree}$ to achieve UTCI decrease in LCZ 6. Even though there is no such $\lambda_{Tree}$ tip off point in LCZ 3 and LCZ 5, a further increase in $\lambda_{Tree}$ above 50 % only provides marginal UTCI cooling during midday in these urban densities (Fig. 6g

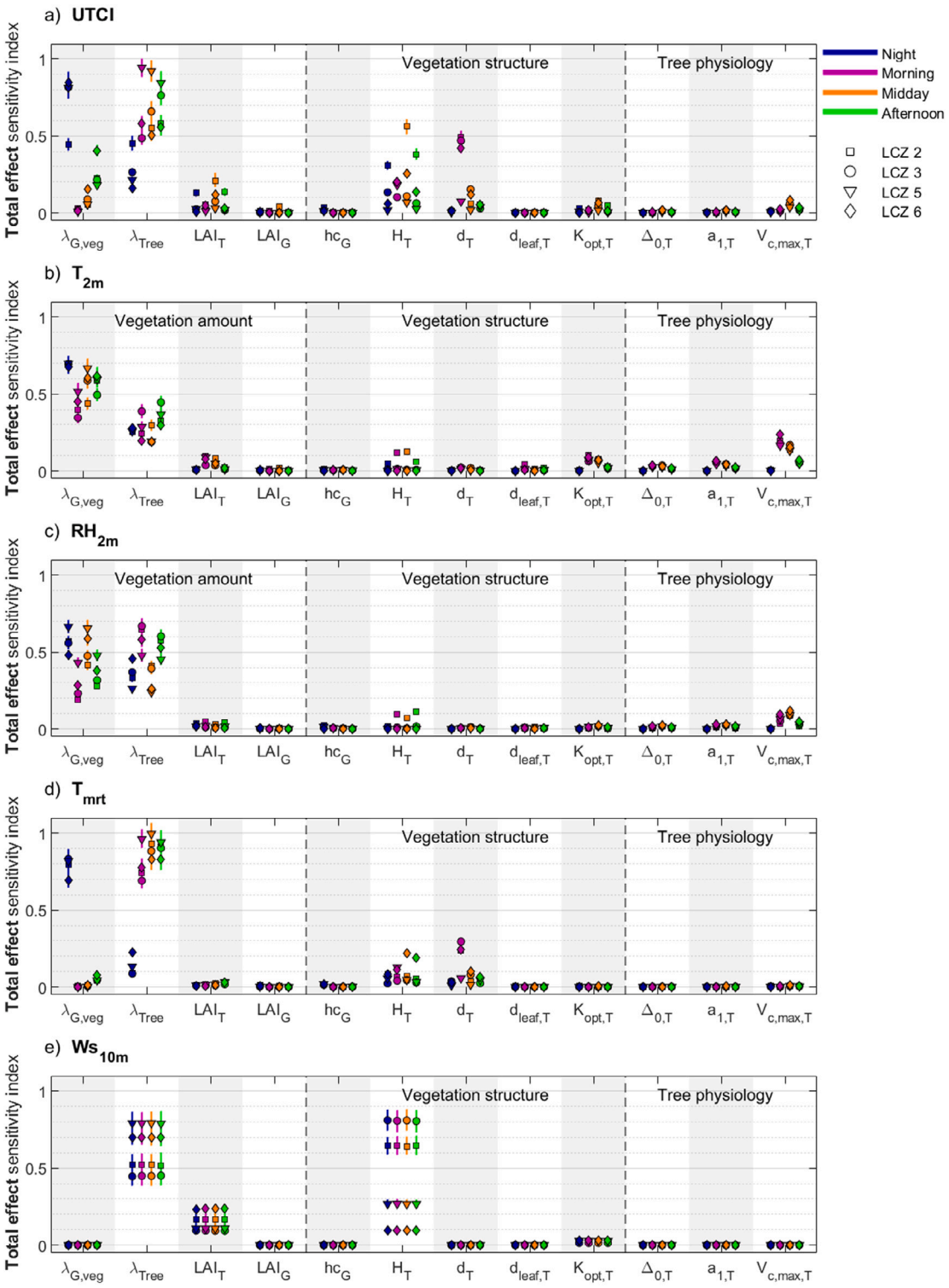


**Fig. 5.** Total effect sensitivity index of the 12 most influential vegetation parameters identified in the EE prescreening. Parameter sensitivity of UTCI, $T_{2m}$, $RH_{2m}$, $T_{mrt}$, and $Ws_{10m}$ is analysed during 4 different times of the day (night, morning, midday, afternoon) in LCZ 2, 3, 5, and 6.

and k). The compact midrise (LCZ 2) urban density overall shows a low potential for UTCI decrease by increasing vegetation fractions. Average UTCI during morning, midday, and afternoon, is at maximum reduced by 0.9 °C considering all combinations of $\lambda_{Tree}$ and $\lambda_{G,veg}$ (Fig. 6a to d). Furthermore, $\lambda_{Tree}$ needs to be increased to a high value to reach such a decrease during morning and midday. In the case of LCZ 2, the effects of vegetation properties on UTCI are almost as relevant as the effect of vegetation cover fraction itself (Fig. 6a to d).

Overall, vegetation can decrease UTCI in a tropical city, and as expected, the highest average UTCI reduction is observed during midday and afternoon hours because of tree shade. However, the average UTCI decrease is fairly small with a maximum of 2.9 °C during midday in LCZ 5 (Fig. 6k). Such a limited effect of vegetation on UTCI is caused by the counteracting effects of $T_{2m}$ and $T_{mrt}$ reduction and humidity ($RH_{2m}$, specific humidity $q_{2m}$) increase (Figure C.11). Figures displaying the $T_{2m}$, $RH_{2m}$, $q_{2m}$ and $T_{mrt}$ changes caused by the change

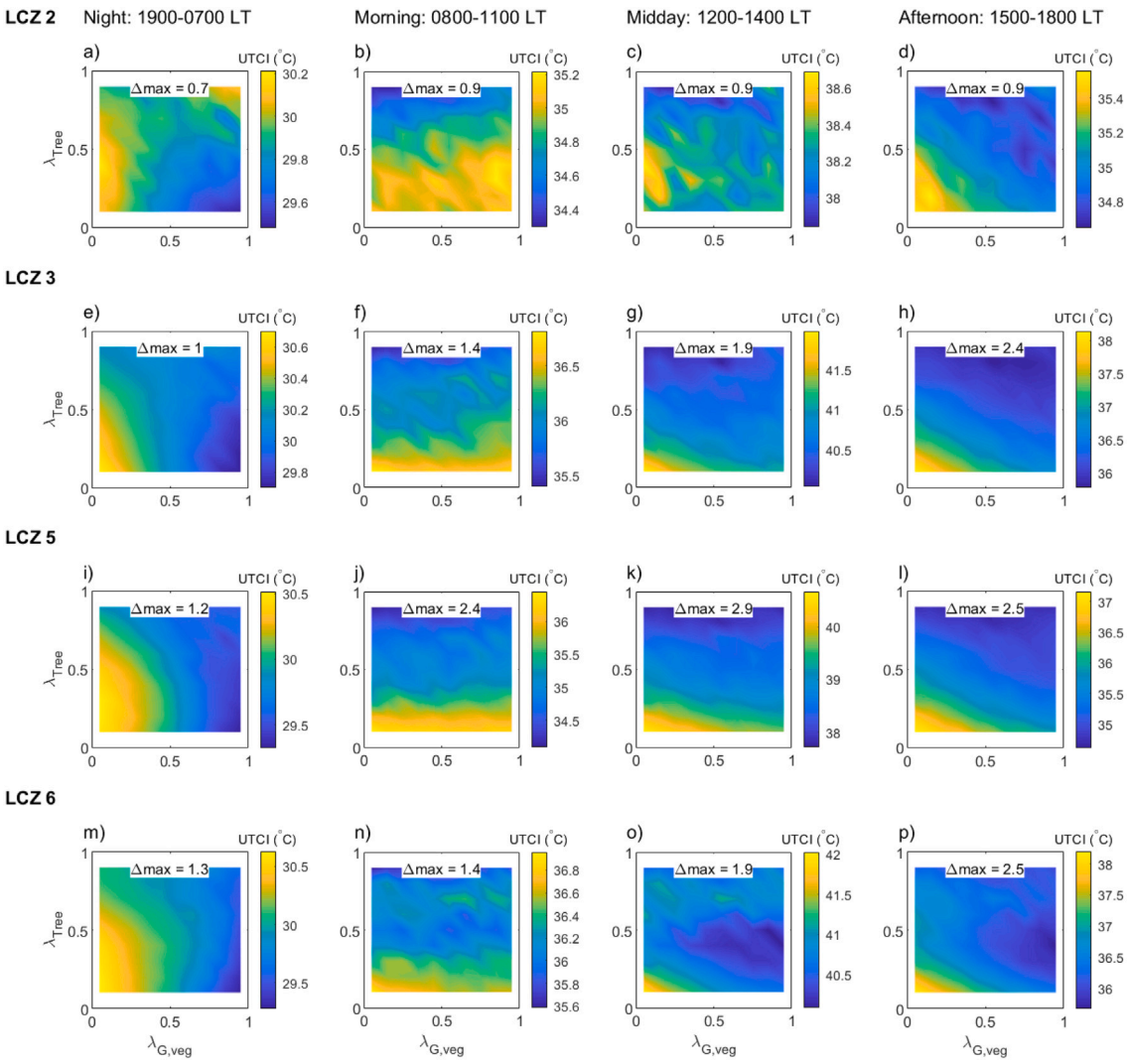


**Fig. 6.** Influence of within canyon ground vegetation fraction, $\lambda_{G,veg}$, and tree canopy fraction, $\lambda_{Tree}$, on UTCI during 4 different times of the day (night, morning, midday, afternoon) in LCZ 2, 3, 5, and 6. Displayed are the average UTCI values over the whole time period (binned according to time of the day) for the specified combinations of $\lambda_{G,veg}$ and $\lambda_{Tree}$. $\Delta max$ is the maximum difference between lowest and highest average UTCI achieved with the different combinations of $\lambda_{G,veg}$ and $\lambda_{Tree}$.

of $\lambda_{Tree}$ and $\lambda_{G,veg}$ are provided in Fig. C.4 to C.7. As the validity of the wind speed alterations caused by trees is uncertain in UT&C's model parameterization, UTCI alterations are also calculated with the average wind speed observed in all simulations grouped by LCZ and time of the day. The results are displayed in Fig. C.10 and show only minor differences.

Unexpectedly, there is no clear pattern of the importance of vegetation properties with $\lambda_{Tree}$ and $\lambda_{G,veg}$ (Fig. 7). In other words, choosing the right plant species can be equally important regardless of the magnitude of $\lambda_{Tree}$ and $\lambda_{G,veg}$.

### 3.5. Vegetation properties that provide cooling during the hottest periods

Mitigating urban heat is especially important during the hottest times of the year and vegetation should be selected strategically to improve OTC during these time periods.

The parameter distribution of the "coolest" model evaluations (Fig. 8 and Fig. C.9) shows that $\lambda_{g,veg}$ has limited influence on UTCI during hot periods, such as midday, while an increase in $\lambda_{Tree}$ reduces UTCI in LCZ 2, 3, and 5, and a $\lambda_{Tree}$ of 40 to 50 % provides highest cooling in LCZ 6 (Fig. 8 and Fig. C.9). Plant physiological parameters that enhance transpiration, such as high values of $V_{c,max,T}$ and $a_{1T}$, and decrease stomatal sensitivity to high vapour pressure deficits, $\Delta_{0,T}$, feature more prominently in scenarios with high cooling during hot periods. Furthermore, a lower optical density, $K_{opt,T}$, has a positive influence during periods of extreme UTCI, most likely due to more uniform access of solar radiation by the tree canopy and therefore, the ability to perform photosynthesis and transpirative cooling deeper in the canopy.

In summary, for the case of Singapore, moderate to high tree cover with highly transpirative tree species provide the highest UTCI reduction during the hottest hours of the year.

## 4. Discussion

### 4.1. UTCI decrease through vegetation and implications for urban planning

Increasing street vegetation cover can decrease UTCI at the local scale in low- to mid-rise urban neighbourhoods in a hot-humid tropical city. However, the effects are in the long-term on average <3 °C as the increase in humidity, both $RH_{2m}$ and $q_{2m}$ due to transpiration, counteracts the decrease in $T_{2m}$ and $T_{mrt}$ (Figure C.11).

An increase in ground or tree vegetation cover provides different UTCI cooling efficiency depending on time of the day and urban density. Hence, urban planners and landscape architects might want to consider the appropriate vegetation type and cover fraction ($\lambda_{G,veg}$,

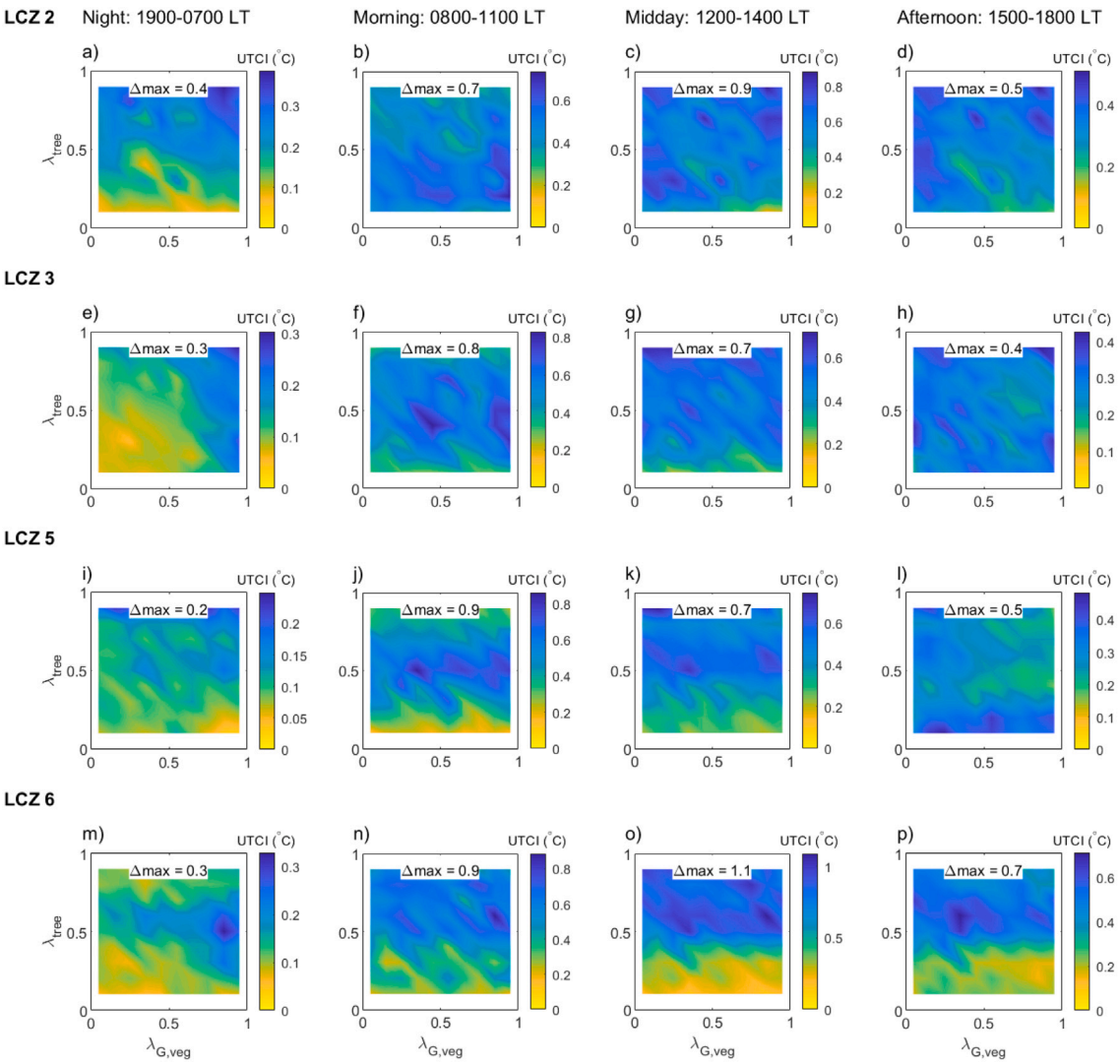


**Fig. 7.** Range of expected UTCI variability (95th–5th percentile) that can be achieved through a change in vegetation properties for a given combination of $\lambda_{G,veg}$ and $\lambda_{Tree}$ during 4 different times of the day (night, morning, midday, afternoon) in LCZ 2, 3, 5, and 6. Results are averaged over the whole time series and within the time bin. *Δmax* is the maximum difference between lowest and highest average UTCI change achieved within the plot.

$\lambda_{Tree}$) according to the intended usage of the urban space to improve its outdoor thermal comfort autonomy [78]. For example, streets experiencing large pedestrian traffic during lunch and early evening hours, would likely benefit from a moderate to high $\lambda_{Tree}$ if they are located in dense low-rise (LCZ3) or open mid-rise areas (LCZ5). However, an increase in $\lambda_{Tree}$ above 50 % only provides minimal further UTCI decrease in LCZ3 and LCZ5 and therefore, a $\lambda_{Tree}$ > 50 % might be considered inefficient, especially if space for tree planting is scarce. On the other hand, urban areas which are mostly occupied at night could benefit from an increase in ground vegetation fraction, $\lambda_{G,veg}$.

Often, urban areas are not just occupied during day or night time but should provide comfortable microclimatic conditions during all times of the day. An increase in $\lambda_{G,veg}$ does not reduce UTCI efficiently during morning and midday hours, but it also does not increase UTCI considerably in most cases, while a larger $\lambda_{Tree}$ does not deter UTCI during night time in the presented simulations, except when combined high $\lambda_{Tree}$ and $\lambda_{G,veg}$ occur. Hence, when a 24 h reduction of UTCI is desired, it is difficult to escape the trivial consideration that ground vegetation and tree cover should and can be combined.

While in the presented simulations, tree cover does not deter UTCI during night time in most scenarios, a modelling study analysing tree cover within urban canyons in Hong Kong found a consistent increase of the OTC index Physiologically Equivalent Temperature (PET) [79] at night due to trees. This increase in PET is caused by the increase in radiation trapping [10]. A previous study analysing the effects of tree-radiation interactions using UT&C in Singapore also modelled an increase in radiation trapping due to tree cover and higher surface and air temperatures at night if evapotranspirative cooling was neglected [36]. However, considering all tree effects, night time air and surface temperatures were decreasing [36].

While the importance of $\lambda_{G,veg}$ and $\lambda_{Tree}$ on UTCI is clear, also vegetation properties can play a non-negligible and sometimes comparable role (e.g. LCZ 2 in Figs. 6 and 7). During hot periods, trees with high photosynthetic activity, high vapour pressure deficit tolerance, and a deeper light penetration throughout the canopy can provide most UTCI decrease, due to high transpiration rates and a low Bowen ratio. However, highly transpirative vegetation might require irrigation during prolonged dry periods to provide such a cooling [80]. Hence, trade-offs between water usage and cooling benefits should be carefully considered in future studies [81].

Furthermore, to ensure sustainable urban planning, the impacts of urban vegetation on the microclimate should not only be analysed in terms of OTC improvement but also consider effects on actual temperature and humidity separately (Fig. C.4 and C.5) as these affect building energy usage for cooling in hot cities, such as Singapore.

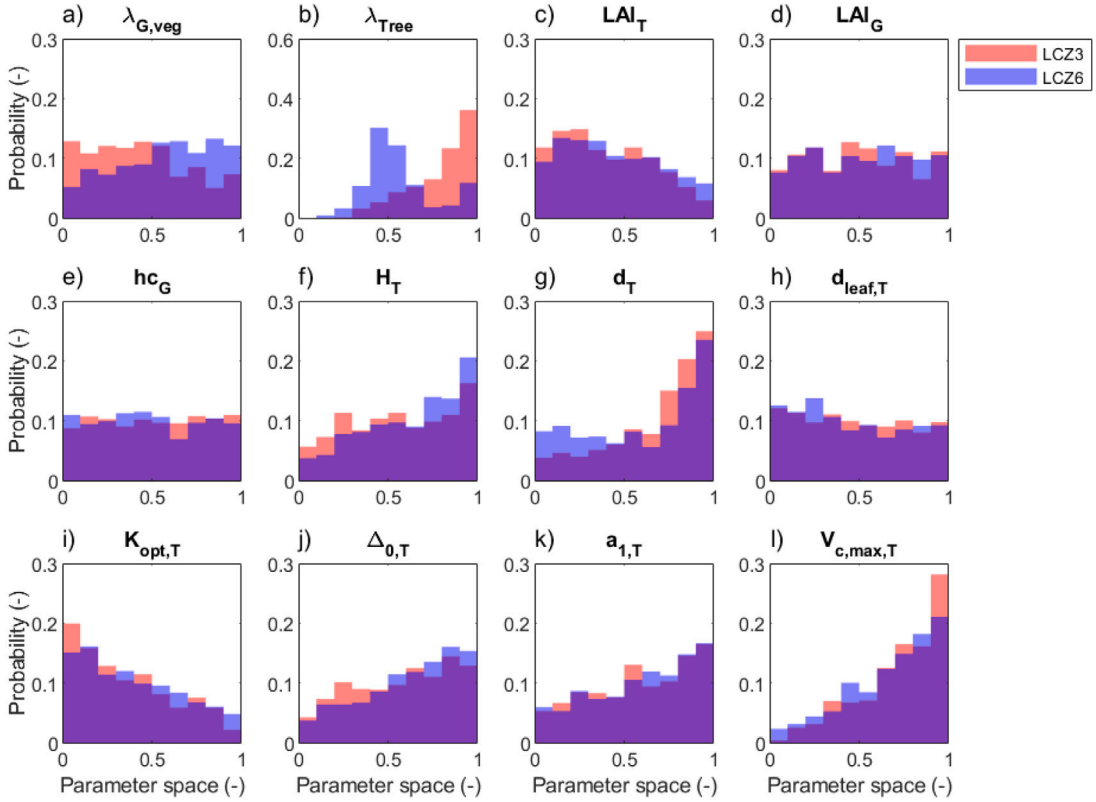


**Fig. 8.** Distribution of vegetation parameters over their total parameter space rescaled uniformly between 0 and 1 for convenience for the 10 % model evaluations with the coolest values of 95th percentile of UTCI cumulative distribution functions as displayed in Fig. C.8. Displayed are the results of LCZ3 and LCZ6, while the results of LCZ2 and LCZ5 can be found in Fig. C.9.

Higher humidity in the air can considerably increase the energy usage of indoor cooling in hot cities [82].

While urban vegetation cover can decrease UTCI in tropical cities, even maximizing vegetation amount is far off from reducing it to the upper limit of the comfortable UTCI range of 26 °C [14]. However, the UTCI comfort assessment scale is not absolute and surveys on pedestrian thermal comfort in Singapore might help in clarifying the actual impact of a given UTCI change. The perception of thermal comfort could indeed differ due to the subjective experience of the outdoor space by people [19].

It is important to note, that the <3 °C predicted UTCI decrease is based on the average conditions a person experiences walking underneath street tree cover (relatively close to the trunk, Section 2.3.2), which might result in shade or sun, depending on the hour of the day and time of the year. Hence, the presented UTCI decrease does not represent the difference of being in shade or sun but is a function of the average shade or sun exposure that can be expected, and therefore much more representative of the long-term impacts of vegetation than a snapshot or single-day analysis often carried out with more complex three-dimensional urban microclimate models. Direct and immediate shade provision has been indeed proven to be an efficient measure for OTC improvement in many studies before [10,12,22,23], as expected from first-order principles.

### 4.2. Implications for urban climate modelling

Recent urban climate model developments have focused on the inclusion of the tree physical structure and its interaction with radiation, while the parameterization of plant transpiration is often simplified [83–85]. Tree physical properties are important when analysing UTCI, however, tree ecophysiology can also play a similarly important role during heat waves or when analysing the effects of urban trees on $T_{2m}$, and $RH_{2m}$ as shown in this study. Hence, a mechanistic representation of tree photosynthesis and transpiration, which is based on plant physiology, is recommended to predict tree-climate interactions under extreme heat and changing environmental conditions and its implementation in future urban climate model developments should be considered.

### 4.3. Limits of interpretation

The presented simulations were performed with a prescribed climatic forcing time series, and thus report local scale effects of vegetation only, but do not include mesoscale feedback. Additionally, it is important to note that the presented parameter sensitivity is based on the local microclimate outputs (UTCI, $T_{2m}$, $RH_{2m}$, $T_{mrt}$). Parameters which appear to be less influential in this study, could play a bigger role when looking at other processes, such as urban energy fluxes or hydrological processes. Hence, parameter sensitivity could be re-evaluated based on the process and also climate of interest in future studies with the same methodology and procedure presented here.

Note that highly local wind speed effects of vegetation are poorly predicted with the current version of UT&C due to a simplified wind profile and lack of consideration of three-dimensional features. The average wind speed effects are shown to be low in our study mostly because of the prevailing calm conditions in Singapore. Hence, this study does not draw any conclusions on the wind speed alterations caused by different vegetation compositions and structural properties. Locations with locally higher wind speed have been reported as more comfortable in Singapore in previous studies [22] and a more detailed representation of three-dimensional wind conditions [e.g., 86,87] could be pursued in detailed urban planning studies.

Finally, vegetation is considered irrigated but effects of water stress could be important for fully evaluating the vegetation benefits [80,81] and are left for detailed future studies on water-stress of urban vegetation.

## 5. Conclusion

The effects of street tree and ground vegetation cover, as well as their structural, optical, interception, and physiological traits on UTCI were analysed in different urban densities and for different hours of the day through a variance based sensitivity analysis. The results show that an increase in urban vegetation cover can reduce UTCI in the tropical city of Singapore by less than 3 °C (long-term average) during midday considering all weather conditions. Further reductions are prevented by a high increase in humidity. Such an increase in humidity does not only decrease thermal comfort but could potentially cause higher energy usage for air conditioning [e.g., 82] and should be analysed carefully in future studies to fully assess the benefits of urban vegetation in hot humid climates.

While $\lambda_{Tree}$ can decrease UTCI during daytime, mostly because of shading, an increase in $\lambda_{G,veg}$ provides more efficient cooling during night time. Whenever possible, $\lambda_{Tree}$ and $\lambda_{G,veg}$ can be combined without any deterioration of UTCI, except for LCZ 2 and LCZ 6 during certain hours of the day. The magnitude of effects vary according to urban density though and urban planners and landscape architects need to consider use and occupational hours of a given urban area to choose the most appropriate vegetation amount and type that can provide UTCI improvement as one-fits-all solutions are unlikely or require a very large vegetation cover at the expense of other uses.

Vegetation traits influence UTCI to a lesser extent than vegetation cover in Singapore. However, considering only the hottest hours, plant traits become more important. Highly transpirative trees provide most UTCI decrease given enough water is available. As vegetation might need irrigation during prolonged dry periods [27], trade-offs between UTCI improvements and water usage should be considered [81].

The presented results and synthesis diagrams are expected to help urban planners and landscape architects on the selection of vegetation amount, type, and traits for improving OTC in tropical cities.

## Declaration of competing interest

The authors declare that they have no known competing financial interests or personal relationships that could have appeared to influence the work reported in this paper.

## Acknowledgements

The research was conducted at the Future Cities Laboratory at the Singapore-ETH Centre, which was established collaboratively between ETH Zurich and Singapore's National Research Foundation (FI370074016) under its Campus for Research Excellence and Technological Enterprise programme. JAA conducted his research under the Cooling Singapore project, funded by Singapore's National Research Foundation (NRF) under its Virtual Singapore programme. Cooling Singapore is a collaborative project led by the Singapore-ETH Centre (SEC), with the Singapore-MIT Alliance for Research and Technology (SMART), TUMCREATE (established by the Technical University of Munich), the National University of Singapore (NUS), the Singapore Management University (SMU), and the Agency for Science, Technology and Research (A*STAR). GM was supported by the "The Branco Weiss Fellowship – Society in Science" administered by ETH Zurich. SF acknowledges the support of the Singapore Ministry of Education Academic Research Fund Tier 1 through the project "Bridging scales from below: The role of heterogeneities in the global water and carbon budgets". The authors would like to thank the Singapore University of Technology and Design (SUTD) for providing the SENSg sensor under its National Science Experiment Programme. The authors would like to thank the Meteorological Service Singapore (MSS) for providing the climatic/meteorological data. This study contains information from Realtime Weather Readings across Singapore accessed on 10th of May 2020 from the National Environment Agency, which is made available under the terms of the Singapore Open Data Licence version 1.0 (https://data.gov.sg/open-data-licence). We gratefully acknowledge Solar Energy Research Institute of Singapore (SERIS) at National University of Singapore (NUS) for providing the solar radiation data. The authors also acknowledge and thank Elliot J.Y. Koh and Yon Sun Tan from SMART who provided important help in the preparation of the sensors set up, and the collection and maintenance of the deployed sensors. The authors further acknowledge and thank Daniel Richards from SEC who provided the scripts to download the climatic/meteorological forcing data from the MSS and Maria Angela Dissegna who provided the high-resolution landcover map of Singapore [33].

## Appendix A. Supplementary data

Supplementary material related to this article can be found online at https://doi.org/10.1016/j.buildenv.2021.107733.

## References

[1] United Nations Department of Economic and Soical Affairs, World urbanization prospects 2018, in: Webpage, 2018, p. 38, https://population.un.org/wup/.

[2] V. Masson-Delmotte, P. Zhai, H.-O. Pörtner, D. Roberts, J. Skea, P. Shukla, A. Pirani, W. Moufouma-Okia, R.P. C. Péan, S. Connors, J. Matthews, Y. Chen, X. Zhou, M. Gomis, E. Lonnoy, T. Maycock, M. Tignor, T. Waterfield (Eds.), Global warming of 1.5° c. An IPCC special report on the impacts of global warming of 1.5° c above pre-industrial levels and related global greenhouse gas emission pathways, in the context of strengthening the global response to the threat of climate change, in: IPCC, 2018.

[3] T.R. Oke, City size and the urban heat island, Atmos. Environ. 7 (7) (1973) 769–779.

[4] D. Li, E. Bou-Zeid, Synergistic interactions between urban heat islands and heat waves : The impact in cities is larger than the sum of its parts *, J. Appl. Meteorol. Climatol. 52 (2013) 2051–2064, http://dx.doi.org/10.1175/JAMC-D-13-02.1.

[5] M.O. Mughal, X.X. Li, T. Yin, A. Martilli, O. Brousse, M.A. Dissegna, L.K. Norford, High-resolution, multilayer modeling of Singapore's urban climate incorporating local climate zones, J. Geophys. Res.: Atmos. 124 (14) (2019) 7764–7785, http://dx.doi.org/10.1029/2018JD029796.

[6] D. Mitchell, C. Heaviside, S. Vardoulakis, C. Huntingford, G. Masato, B. P Guillod, P. Frumhoff, A. Bowery, D. Wallom, M. Allen, Attributing human mortality during extreme heat waves to anthropogenic climate change, Environ. Res. Lett. 11 (2016) 074006, http://dx.doi.org/10.1088/1748-9326/11/7/074006.

[7] C. Mora, B. Dousset, I.R. Caldwell, F.E. Powell, R.C. Geronimo, C.R. Bielecki, C.W.W. Counsell, B.S. Dietrich, E.T. Johnston, L.V. Louis, M.P. Lucas, M.M. Mckenzie, A.G. Shea, H. Tseng, T.W. Giambelluca, L.R. Leon, E. Hawkins, C. Trauernicht, Global risk of deadly heat, Nature Clim. Change (June) (2017) http://dx.doi.org/10.1038/NCLIMATE3322.

[8] Z.H. Wang, X. Zhao, J. Yang, J. Song, Cooling and energy saving potentials of shade trees and urban lawns in a desert city, Appl. Energy 161 (2016) 437–444, http://dx.doi.org/10.1016/j.apenergy.2015.10.047.

[9] L.V. de Abreu-Harbich, L.C. Labaki, A. Matzarakis, Effect of tree planting design and tree species on human thermal comfort in the tropics, Landsc. Urban Plan. 138 (2015) 99–109, http://dx.doi.org/10.1016/j.landurbplan.2015.02.008.

[10] T.E. Morakinyo, L. Kong, K.K.L. Lau, C. Yuan, E. Ng, A study on the impact of shadow-cast and tree species on in-canyon and neighborhood's thermal comfort, Build. Environ. 115 (2017) 1–17, http://dx.doi.org/10.1016/j.buildenv.2017.01.005.

[11] G. Manoli, S. Fatichi, M. Schläpfer, K. Yu, T.W. Crowther, N. Meili, P. Burlando, G.G. Katul, E. Bou-Zeid, Magnitude of urban heat islands largely explained by climate and population, Nature 573 (7772) (2019) 55–60, http://dx.doi.org/10.1038/s41586-019-1512-9.

[12] A.M. Coutts, E.C. White, N.J. Tapper, J. Beringer, S.J. Livesley, Temperature and human thermal comfort effects of street trees across three contrasting street canyon environments, Theor. Appl. Climatol. 124 (1–2) (2016) 55–68, http://dx.doi.org/10.1007/s00704-015-1409-y.

[13] X.P. Song, D. Richards, P. Edwards, P.Y. Tan, Benefits of trees in tropical cities, Sci. Total Environ. 356 (6344) (2017) 1241, http://dx.doi.org/10.1126/science.aan6642.

[14] P. Bröde, D. Fiala, K. Błażejczyk, I. Holmér, G. Jendritzky, B. Kampmann, B. Tinz, G. Havenith, Deriving the operational procedure for the Universal Thermal Climate Index (UTCI), Int. J. Biometeorol. 56 (3) (2012) 481–494, http://dx.doi.org/10.1007/s00484-011-0454-1.

[15] G. Jendritzky, R. de Dear, G. Havenith, UTCI-why another thermal index? Int. J. Biometeorol. 56 (3) (2012) 421–428, http://dx.doi.org/10.1007/s00484-011-0513-7.

[16] I. Charalampopoulos, A comparative sensitivity analysis of human thermal comfort indices with generalized additive models, Theor. Appl. Climatol. 137 (1–2) (2019) 1605–1622, http://dx.doi.org/10.1007/s00704-019-02900-1.

[17] S. Provençal, O. Bergeron, R. Leduc, N. Barrette, Thermal comfort in Quebec City, Canada: sensitivity analysis of the UTCI and other popular thermal comfort indices in a mid-latitude continental city, Int. J. Biometeorol. 60 (4) (2016) 591–603, http://dx.doi.org/10.1007/s00484-015-1054-2.

[18] I. Knez, S. Thorsson, Thermal, emotional and perceptual evaluations of a park: Cross-cultural and environmental attitude comparisons, Build. Environ. 43 (9) (2008) 1483–1490, http://dx.doi.org/10.1016/j.buildenv.2007.08.002.

[19] W. Klemm, B.G. Heusinkveld, S. Lenzholzer, M.H. Jacobs, Psychological and physical impact of urban green spaces on outdoor thermal comfort during summertime in The Netherlands, Build. Environ. 83 (2015) 120–128, http://dx.doi.org/10.1016/j.buildenv.2014.05.013.

[20] C.K.C. Lam, A.J. Gallant, N.J. Tapper, Perceptions of thermal comfort in heatwave and non-heatwave conditions in melbourne, Australia, Urban Clim. 23 (2018) 204–218, http://dx.doi.org/10.1016/j.uclim.2016.08.006.

[21] S.L. Heng, W.T. Chow, How 'hot' is too hot? Evaluating acceptable outdoor thermal comfort ranges in an equatorial urban park, Int. J. Biometeorol. (2019) 801–816, http://dx.doi.org/10.1007/s00484-019-01694-1.

[22] W.T. Chow, S.N.A.B.A. Akbar, S.L. Heng, M. Roth, Assessment of measured and perceived microclimates within a tropical urban forest, Urban Forestry Urban Green. 16 (2016) 62–75, http://dx.doi.org/10.1016/j.ufug.2016.01.010.

[23] A. Middel, N. Selover, B. Hagen, N. Chhetri, Impact of shade on outdoor thermal comfort—a seasonal field study in tempe, arizona, Int. J. Biometeorol. 60 (12) (2016) 1849–1861, http://dx.doi.org/10.1007/s00484-016-1172-5.

[24] NEA, National environment agency of Singapore, http://www.weather.gov.sg/climate-climate-of-singapore/, august 2020, 2020, URL http://www.weather.gov.sg/climate-climate-of-singapore/.

[25] H. Staiger, G. Laschewski, A. Matzarakis, Selection of appropriate thermal indices for applications in human biometeorological studies, Atmosphere 10 (1) (2019) 1–15, http://dx.doi.org/10.3390/atmos10010018.

[26] Y.C. Chen, A. Matzarakis, Modified physiologically equivalent temperature—basics and applications for western European climate, Theor. Appl. Climatol. 132 (3–4) (2018) 1275–1289, http://dx.doi.org/10.1007/s00704-017-2158-x.

[27] N. Meili, G. Manoli, P. Burlando, E. Bou-Zeid, W.T. Chow, A. Coutts, E. Daly, K. Nice, M. Roth, N. Tapper, E. Velasco, E. Vivoni, S. Fatichi, An urban ecohydrological model to quantify the effect of vegetation on urban climate and hydrology (UT&C v1.0), Geosci. Model Dev. 13 (2020) 335–362, http://dx.doi.org/10.5194/gmd-2019-225.

[28] J. Kattge, G. Bönisch, S. Díaz, S. Lavorel, I.C. Prentice, P. Leadley, S. Tautenhahn, G.D. Werner, T. Aakala, M. Abedi, et al., TRY plant trait database – enhanced coverage and open access, Global Change Biol. 26 (1) (2020) 119–188, http://dx.doi.org/10.1111/gcb.14904.

[29] K.A. Nice, A.M. Coutts, N.J. Tapper, Development of the VTUF-3D v1.0 urban micro-climate model to support assessment of urban vegetation influences on human thermal comfort, Urban Clim. (2018) 1–25, http://dx.doi.org/10.1016/j.uclim.2017.12.008.

[30] S. Fatichi, V.Y. Ivanov, E. Caporali, A mechanistic ecohydrological model to investigate complex interactions in cold and warm water-controlled environments : 2 . spatiotemporal analyses, J. Adv. Modelling Earth Syst. 4 (2012) 1–22, http://dx.doi.org/10.1029/2011MS000087.

[31] C. Pappas, S. Fatichi, S. Leuzinger, A. Wolf, P. Burlando, Sensitivity analysis of a process-based ecosystem model: Pinpointing parameterization and structural issues, J. Geophys. Res.: Biogeosci. 118 (2) (2013) 505–528, http://dx.doi.org/10.1002/jgrg.20035.

[32] J. Ching, G. Mills, B. Bechtel, L. See, J. Feddema, X. Wang, C. Ren, O. Brorousse, A. Martilli, M. Neophytou, P. Mouzourides, I. Stewart, A. Hanna, E. Ng, M. Foley, P. Alexander, D. Aliaga, D. Niyogi, A. Shreevastava, P. Bhalachandran, V. Masson, J. Hidalgo, J. Fung, M. Andrade, A. Baklanov, W. Dai, G. Milcinski, M. Demuzere, N. Brunsell, M. Pesaresi, S. Miao, Q. Mu, F. Chen, N. Theeuwesits, WUDAPT: An urban weather, climate, and environmental modeling infrastructure for the anthropocene, Bull. Am. Meteorol. Soc. 99 (9) (2018) 1907–1924, http://dx.doi.org/10.1175/BAMS-D-16-0236.1.

[33] M.A. Dissegna, T. Yin, S. Wei, D. Richards, A. Grêt-Regamey, 3-D reconstruction of an urban landscape to assess the influence of vegetation in the radiative budget, Forests 10 (8) (2019) 1–19, http://dx.doi.org/10.3390/f10080700.

[34] R.W. Macdonald, R.F. Griffiths, D.J. Hall, An improved method for the estimation of surface roughness of obstacle arrays, Atmos. Environ. 32 (11) (1998) 1857–1864.

[35] C.W. Kent, S. Grimmond, D. Gatey, Aerodynamic roughness parameters in cities: Inclusion of vegetation, J. Wind Eng. Ind. Aerodyn. 169 (December 2016) (2017) 168–176, http://dx.doi.org/10.1016/j.jweia.2017.07.016.

[36] N. Meili, G. Manoli, P. Burlando, J. Carmeliet, W.T. Chow, Andrew, M. Coutts, M. Roth, E. Velasco, R.V. Enrique, F. Simone, Tree effects on urban microclimate: diurnal, seasonal, and climatic temperature differences explained by separating radiation, evapotranspiration, and roughness effects , Urban Forestry Urban Green. (December) (2020) 126970, http://dx.doi.org/10.1016/j.ufug.2020.126970.

[37] V. Masson, A physically-based scheme for the urban energy budget in atmospheric models, Bound.-Lay. Meteorol. 94 (September 1999) (2000) 357–397.

[38] V. Mahat, D.G. Tarboton, N.P. Molotch, Testing above- and below-canopy representations of turbulent fluxes in an energy balance snowmelt model, Water Resour. Res. 49 (2013) 1107–1122, http://dx.doi.org/10.1002/wrcr.20073.

[39] UTCI, 2020, http://www.utci.org/.

[40] M. Roth, C. Jansson, E. Velasco, Multi-year energy balance and carbon dioxide fluxes over a residential neighbourhood in a tropical city, Int. J. Climatol. (2016) http://dx.doi.org/10.1002/joc.4873.

[41] D.R. Richards, T.K. Fung, R.N. Belcher, P.J. Edwards, Differential air temperature cooling performance of urban vegetation types in the tropics, Urban Forestry Urban Green. 50 (June 2019) (2020) doi:10.1016/j.ufug.2020.126651.

[42] E. Velasco, M. Roth, S.H. Tan, M. Quak, S.D.A. Nabarro, L. Norford, The role of vegetation in the CO2 flux from a tropical urban neighbourhood, Atmos. Chem. Phys. 13 (2013) 10185–10202, http://dx.doi.org/10.5194/acp-13-10185-2013.

[43] Google, Google maps, 2020, URL https://www.google.com/maps/place/Singapore/@1.2866421,103.8328658,5811m.

[44] S. Fatichi, V.Y. Ivanov, E. Caporali, Simulation of future climate scenarios with a weather generator, Adv. Water Resour. 34 (4) (2011) 448–467, http://dx.doi.org/10.1016/j.advwatres.2010.12.013.

[45] S. Fatichi, V.Y. Ivanov, E. Caporali, A mechanistic ecohydrological model to investigate complex interactions in cold and warm water-controlled environments : 1 . Theoretical framework and plot-scale analysis, J. Adv. Modelling Earth Syst. 4 (2012) 1–31, http://dx.doi.org/10.1029/2011MS000086.

[46] A.K. Quah, M. Roth, Diurnal and weekly variation of anthropogenic heat emissions in a tropical city, Singapore, Atmos. Environ. 46 (2012) 92–103, http://dx.doi.org/10.1016/j.atmosenv.2011.10.015.

[47] C.J. Willmott, Some Comments on the Evaluation of Model Performance, Bulletin American Meteorological Society, 1982.

[48] I.D. Stewart, T.R. Oke, Local Climate Zones for Urban Temperature Studies, American Meteorological Society, 2012, http://dx.doi.org/10.1175/BAMS-D-11-00019.1.

[49] K.Y. Chong, H.T.W. Tan, R.T. Corlett, A Checklist of the Total Vascular Plant Flora of Singapore, 2009.

[50] R.T. Corlett, Urban biodiversity, Trop. Xishuangbanna Bot. Garden (2011) (in Singapore).

[51] K. Chong, H.T. Tan, R.T. Corlett, A summary of the total vascular plant flora of Singapore, Gardens' Bull. Singapore 63 (1&2) (2011) 197–204.

[52] P. Edwards, Z. Drillet, D.R. Richards, T. Fung, X.P. Song, R.A.T. Leong, L.Y.F. Gaw, A.T.K. Yee, S.A. Quazi, S. Ghosh, K.W.J. Chua, Ecosystem Services in Urban Landscapes: Benefits of Tropical Urban Vegetation, Singapore-ETH Centre, Future Cities Laboratory, 2020.

[53] A. Iio, K. Hikosaka, N.P. Anten, Y. Nakagawa, A. Ito, Global dependence of field-observed leaf area index in woody species on climate: A systematic review, Global Ecol. Biogeogr. 23 (3) (2014) 274–285, http://dx.doi.org/10.1111/geb.12133.

[54] P.Y. Tan, A. Sia, Leaf Area Index of Tropical Plants: a Guidebook on Its Use in the Calculation of Green Plot Ratio, Singapore, Centre of Urban Greenery and Ecology, 2009.

[55] M. Simard, N. Pinto, J.B. Fisher, A. Baccini, Mapping forest canopy height globally with spaceborne lidar, J. Geophys. Res.: Biogeosci. 116 (4) (2011) 1–12, http://dx.doi.org/10.1029/2011JG001708.

[56] I.J. Wright, N. Dong, V. Maire, I.C. Prentice, M. Westoby, S. Díaz, R.V. Gallagher, B.F. Jacobs, R. Kooyman, E.A. Law, M.R. Leishman, Ü. Niinemets, P.B. Reich, L. Sack, R. Villar, H. Wang, P. Wilf, Global climatic drivers of leaf size, Science 357 (6354) (2017) 917–921, http://dx.doi.org/10.1126/science.aal4760.

[57] M.A. White, P.E. Thornton, S.W. Running, R.R. Nemani, Parameterization and sensitivity analysis of the BIOME–bgc terrestrial ecosystem model: Net primary production controls, Earth Interact. 4 (3) (2000) 1–85, http://dx.doi.org/10.1175/1087-3562(2000)004<0003:pasaot>2.0.co;2.

[58] C.J. Houldcroft, W.M. Grey, M. Barnsley, C.M. Taylor, S.O. Los, P.R. North, New vegetation albedo parameters and global fields of soil background albedo derived from MODIS for use in a climate model, J. Hydrometeorol. 10 (1) (2009) 183–198, http://dx.doi.org/10.1175/2008JHM1021.1.

[59] S. Harshan, M. Roth, E. Velasco, M. Demuzere, Evaluation of an urban land surface scheme over a tropical suburban neighborhood, Theor. Appl. Climatol. (2017) 1–20, http://dx.doi.org/10.1007/s00704-017-2221-7.

[60] J.-f. Mahfouf, B. Jacquemin, A study of rainfall interception using a land surface parameterization for mesoscale meteorological models, J. Appl. Meteorol. 28 (1989) 1282.

[61] S. Fatichi, C. Pappas, Constrained variability of modeled T:ET ratio across biomes, Geophys. Res. Lett. 44 (13) (2017) 6795–6803, http://dx.doi.org/10.1002/2017GL074041.

[62] R. LEUNING, A critical appraisal of a combined stomatal-photosynthesis model for C3 plants, Plant Cell Environ. 18 (4) (1995) 339–355, http://dx.doi.org/10.1111/j.1365-3040.1995.tb00370.x.

[63] S.D. Wullschleger, Biochemical limitations to carbon assimilation in C3 plants - a retrospective analysis of the A/Ci curves from 109 species, J. Exp. Bot. 44 (5) (1993) 907–920, http://dx.doi.org/10.1093/jxb/44.5.907.

[64] J. Kattge, W. Knorr, T. Raddatz, C. Wirth, Quantifying photosynthetic capacity and its relationship to leaf nitrogen content for global-scale terrestrial biosphere models, Global Change Biol. 15 (4) (2009) 976–991, http://dx.doi.org/10.1111/j.1365-2486.2008.01744.x.

[65] F. Campolongo, J. Cariboni, A. Saltelli, An effective screening design for sensitivity analysis of large models, Environ. Modelling Softw. 22 (10) (2007) 1509–1518, http://dx.doi.org/10.1016/j.envsoft.2006.10.004.

[66] A. Saltelli, S. Tarantola, F. Campolongo, M. Ratto, Sensitivity Analysis in Practice: a Guide to Assessing Scientific Models (Google Ebook), 2004, p. 219.

[67] M.D. Morris, Factorial sampling plans for preliminary computational experiments, Technometrics 33 (2) (1991) 161–174, http://dx.doi.org/10.1080/00401706.1991.10484804.

[68] I. Sobol, Sensitivity analysis for nonlinear mathematical models, Math. Model Comput. Exp. 1 (4) (1993) 407–414, 1061-7590/93/04407-008$9.00.

[69] A. Saltelli, P. Annoni, I. Azzini, F. Campolongo, M. Ratto, S. Tarantola, Variance based sensitivity analysis of model output. Design and estimator for the total sensitivity index, Comput. Phys. Comm. 181 (2) (2010) 259–270, http://dx.doi.org/10.1016/j.cpc.2009.09.018.

[70] F. Pianosi, F. Sarrazin, T. Wagener, A matlab toolbox for global sensitivity analysis, Environ. Modelling Softw. 70 (2015) 80–85, http://dx.doi.org/10.1016/j.envsoft.2015.04.009.

[71] G. Archer, A. Saltelli, I. Sobol, Sensitivity measures, ANOVAlike techniques and the use of bootstrap, J. Stat. Computat. Simul 2 (58) (1997) 99–120.

[72] T. Homma, A. Saltelli, Importance measures in global sensitivity analysis of nonlinear models, Reliab. Eng. Syst. Saf. 52 (1) (1996) 1–17, http://dx.doi.org/10.1016/0951-8320(96)00002-6.

[73] A. Saltelli, Making best use of model evaluations to compute sensitivity indices, Comput. Phys. Comm. 145 (2) (2002) 280–297, http://dx.doi.org/10.1016/S0010-4655(02)00280-1.

[74] M.J.W. Jansen, Analysis of variance designs for model output, Comput. Phys. Comm. 117 (1996) 35–43.

[75] I.M. Sobol, S. Tarantola, D. Gatelli, S. Kucherenko, W. Mauntz, Estimating the approximation error when fixing unessential factors in global sensitivity analysis, Reliab. Eng. Syst. Saf. 92 (7) (2007) 957–960.

[76] I. Sobol, On the distribution of points in a cube and the approximate evaluation of integrals, Comput. Math. Math. Phys. 7 (4) (1967) 86–112.

[77] I. Sobol, Uniformly distributed sequences with an additional uniform property, USSR Comput. Math. Math. Phys. 16 (5) (1976) 236–242, http://dx.doi.org/10.1016/0041-5553(76)90154-3.

[78] N. Nazarian, J.A. Acero, L. Norford, Outdoor thermal comfort autonomy: Performance metrics for climate-conscious urban design, Build. Environ. 155 (March) (2019) 145–160, http://dx.doi.org/10.1016/j.buildenv.2019.03.028.

[79] P. Höppe, The physiological equivalent temperature - a universal index for the biometeorological assessment of the thermal environment, Int. J. Biometeorol. 43 (2) (1999) 71–75, http://dx.doi.org/10.1007/s004840050118.

[80] A.M. Broadbent, A.M. Coutts, N.J. Tapper, M. Demuzere, The cooling effect of irrigation on urban microclimate during heatwave conditions, Urban Clim. 23 (2018) 309–329, http://dx.doi.org/10.1016/j.uclim.2017.05.002.

[81] C. Wang, Z.-H. Wang, J. Yang, Urban water capacity: Irrigation for heat mitigation, Comput. Environ. Urban Syst. 78 (August) (2019) 101397, http://dx.doi.org/10.1016/j.compenvurbsys.2019.101397.

[82] J. Fonseca, A. Schlueter, Daily enthalpy gradients and the effects of climate change on the thermal energy demand of buildings in the United States, Appl. Energy 262 (September 2019) (2020) 114458, http://dx.doi.org/10.1016/j.apenergy.2019.114458.

[83] Y.-H. Ryu, E. Bou-Zeid, Z.-H. Wang, J.A. Smith, Realistic representation of trees in an urban canopy model, Bound.-Lay. Meteorol. 159 (2) (2016) 193–220, http://dx.doi.org/10.1007/s10546-015-0120-y.

[84] E.C. Redon, A. Lemonsu, V. Masson, B. Morille, M. Musy, Implementation of street trees within the solar radiative exchange parameterization of TEB in SURFEX v8.0, Geosci. Model Dev. 10 (2017) 385–411, http://dx.doi.org/10.5194/gmd-10-385-2017.

[85] E.S. Krayenhoff, T. Jiang, A. Christen, A. Martilli, T.R. Oke, B.N. Bailey, N. Nazarian, J.A. Voogt, M.G. Giometto, A. Stastny, B.R. Crawford, A multi-layer urban canopy meteorological model with trees (BEP-tree): Street tree impacts on pedestrian-level climate, Urban Clim. 32 (2020) 100590, http://dx.doi.org/10.1016/j.uclim.2020.100590.

[86] S. Saneinejad, P. Moonen, J. Carmeliet, Coupled CFD, radiation and porous media model for evaluating the micro-climate in an urban environment, J. Wind Eng. Ind. Aerodyn. 128 (2014) 1–11, http://dx.doi.org/10.1016/j.jweia.2014.02.005.

[87] L. Manickathan, T. Defraeye, J. Allegrini, D. Derome, J. Carmeliet, Parametric study of the influence of environmental factors and tree properties on the transpirative cooling effect of trees, Agricult. Forest Meteorol. 248 (October 2017) (2018) 259–274, http://dx.doi.org/10.1016/j.agrformet.2017.10.014.